STATE OF ILLINOIS

ADLAI E. STEVENSON, *Governor*

STUDIES OF THUNDERSTORM RAINFALL WITH DENSE RAINGAGE NETWORKS AND RADAR

H. E. HUDSON, JR., G. E. STOUT,
F. A. HUFF.

DEPARTMENT OF REGISTRATION AND EDUCATION

C. HOBART ENGLE, *Director*

STATE WATER SURVEY DIVISION

A. M. BUSWELL, *Chief*

URBANA, ILLINOIS

(Printed By Authority of State of Illinois)

CONTENTS

STUDIES OF THUNDERSTORM RAINFALL WITH DENSE RAINGAGE NETWORKS AND RADAR*

by

H. E. Hudson, Jr., Head
G. E. Stout and F. A. Huff, Meteorologists
Engineering Subdivision
State Water Survey
Urbana, Illinois

SUMMARY

The results of three years' work on concentrated raingage networks and on radar rainfall extent and intensity measurements are described. Thunderstorm rainfall is shown to be multicellular, so that the application of area-depth data is more complex than is usually assumed.

The orientation, duration, and path of storm cells are shown to have marked effects on area-depth curves for a given basin. Data on area-depth relationships are presented for networks of 5.2-, 95-, and 280-square-mile areas.

Effects of gage density on mean rainfall errors are investigated. Heaviest storms were found to be associated with cold fronts.

Theory and development of radar for rainfall measurement are reviewed. Available methods of measuring rainfall by radar are discussed. Data collected in the study on radar signal strength and rainfall intensity are presented and analyzed using a new analytical approach. It is concluded that radar is able to depict rainfall extent better than raingaging, and that radar can measure rainfall intensities as well as the raingage networks generally used.

INTRODUCTION

The standard raingage that has provided engineers with limited rainfall data may be replaced in this age of electronics. Radar, a high frequency radio device which became a reality during World War II, has since been used by the Illinois Water Survey to detect, track and quantitatively measure rainfall over the northern half of Illinois. The detection and tracking of rainfall was recognized by the military users of radar, but has not been deeply explored for its application in the field of hydro-meteorology.

Present raingaging techniques do not provide the accuracy desired by engineers and meteorologists. On the smaller watersheds under study in Illinois prior to 1948, gage densities of 15 square miles per gage were employed, but large differences of rainfall were encountered, especially when the precipitation occurred in the form of local showers or thunderstorms. In Illinois the bulk of the year's precipitation comes from such storms. If the density of the network was increased tenfold, it would not be able to depict the details of rainfall from small storms. Furthermore, the task of collecting and compiling all the data would be huge.

When rainmaking activities boomed in 1947, the Survey gathered data on this new water resource of Illinois. Interest was so great that the Pfister Hybrid Corn Company of El Paso, Illinois, in cooperation with the Water Survey, organized a program to evaluate the possibilities of induced precipitation. A war-surplus AN/APS-15 radar set was purchased by the cooperating group to be used for the tracking of both aircraft and rainfall during any rainmaking attempts. Gradually, while rainmaking did not seem to prove necessary in Illinois, the utility of the radar unit at El Paso for portraying the areal extent of the rainfall became evident. It was thought that the quantity of rainfall could be determined as well as the areal extent with this equipment. Practically it appeared that a radar scanning a radius of 70 miles or 15, 000 square miles could also give the quantity of rainfall deposited in that area and thus supplement or even eliminate the standard raingage.

As a check on the possibilities of the cloud seeding work planned, a raingage network was installed in the vicinity of El Paso in Spring 1948. This network, continued in revised form in 1949 and 1950, proved of little value for radar studies, due to "ground clutter" appearing on the radar scope, caused by trees and structures close to the radar. However, the El Paso network did produce much thunderstorm rainfall data.

*This paper was presented at the Houston Convention of the American Society of Civil Engineers on February 22, 1951.

GAGE NETWORKS USED

Three raingage networks were available for the past three years to enable analysis of the character of the storms involved in these studies.

These networks are shown in Figure 1-3. The 280-square-mile network in the vicinity of El Paso, Illinois (Figure 1) was initiated in the spring of 1948. It was reorganized at the close of the 1949 thunderstorm season. Beginning in the spring of 1950, the 95-square-mile Panther Creek network (Figure 2) has been operated in conjunction with a detailed hydrologic study on that watershed. To obtain more rainfall data for this type of watershed, a different area of the same size and shape was chosen from the 280-square-mile network in the area of maximum gage density. There are no distinct topographic or climatic features in the region. The superimposed area is shown by the dashed outline in Figure 1. The 5. 2-square-mile network, located on Boneyard Creek at Champaign-Urbana, Illinois, is shown in Figure 3. This network has been operated since the fall of 1948 in cooperation with the Civil Engineering Department, University of Illinois.

The 280-square-mile area gaged in 1948-1949 contained a total of 29 stick and 17 recording gages, or an average of one gage per 6. 1 square miles. Within this area was the 95-square-mile area that had 14 stickand 6 recording gages during the 1948-1949 seasons, corresponding to an average of one gage per 4. 75 square miles. During the 1950 thunderstorm season, 30 stick and 26 recording gages were located on or in the vicinity of the 95-square-mile watershed. The Boneyard watershed included 7 recording gages or an average of one gage per 0. 7 square mile.

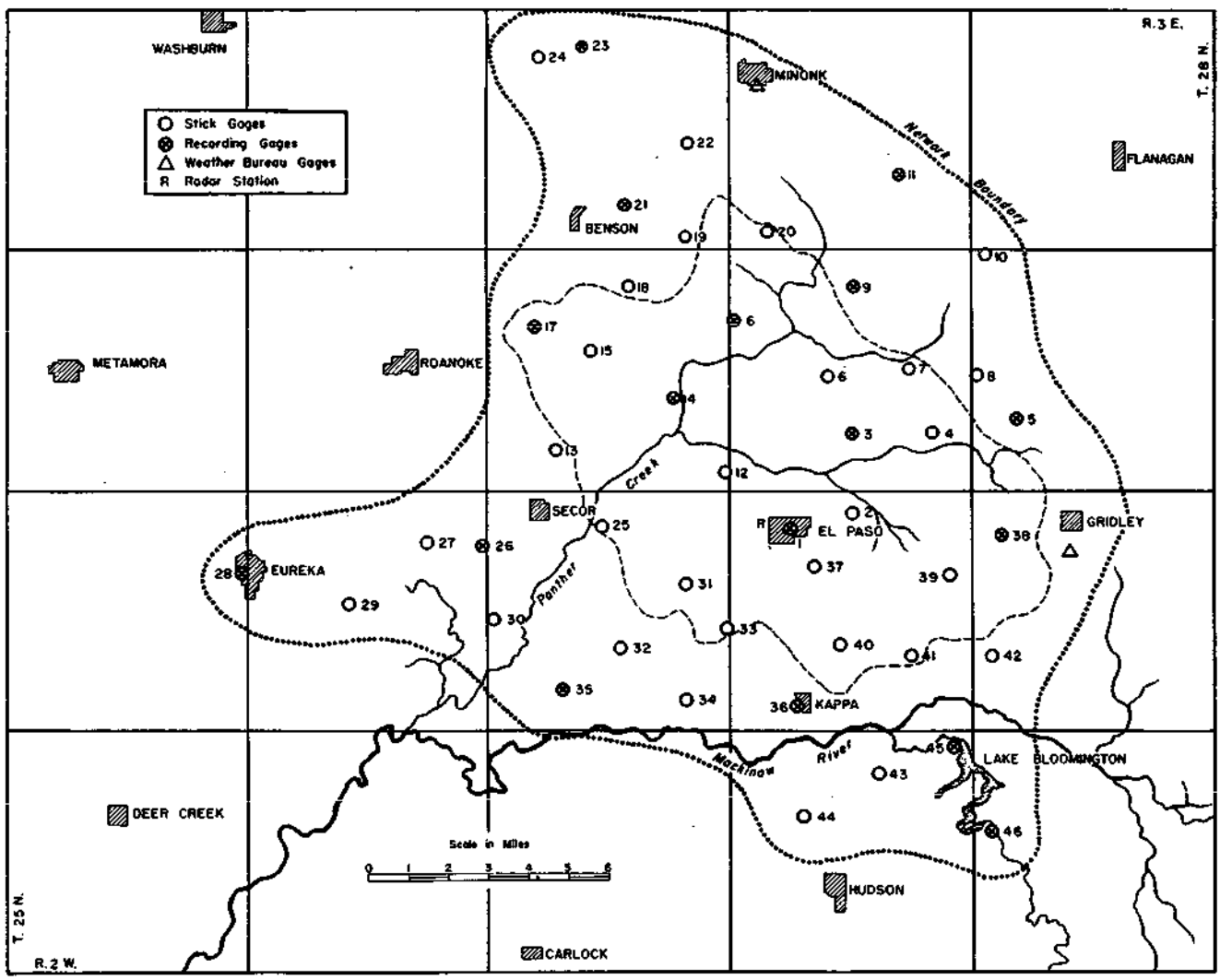

FIG. 1. 1948-49 PANTHER CREEK RAINGAGE NETWORK.

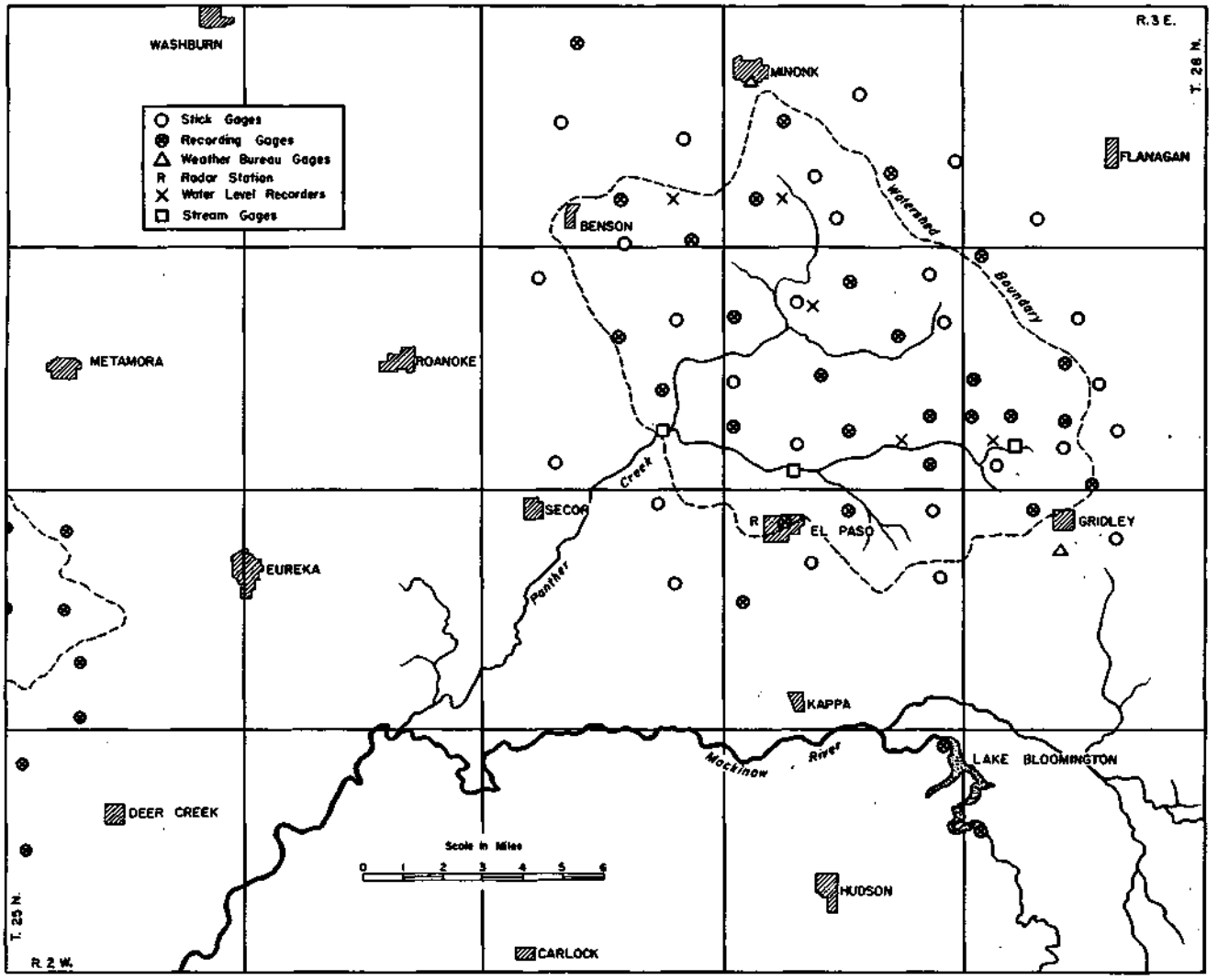

FIG. 2. 1950 PANTHER CREEK RAINGAGE NETWORK.

AREA-DEPTH RELATIONSHIPS

For many engineering design purposes, a detailed knowledge of duration-area-depth relationships for small areas is essential. Very few published data are available for areal units under 100 square miles. Raingage networks of sufficient density to permit area-depth extrapolations with a reasonable degree of accuracy to such small areas have seldom existed. Rainfall data, collected on three networks of 5.2, 95, and 280 square miles in Central Illinois, have been analyzed in an attempt to furnish some concrete information on the characteristics of the area-depth curve for small watersheds in thunderstorm rainfall. The present analysis is concerned chiefly with the 95-square-mile basin for which three years' data are available. More limited data for the 280- and 5. 2-square-mile areas have been used to supplement this study. Only data for the thunderstorm season, May-September, have been used in the analysis.

Effect of Gage Density on Area-Depth Curve. During the summer of 1950, 40 gages were located on or within the boundaries of the 95-square-mile Panther Creek watershed. For the 1948-1949 seasons, when a much larger area was gaged,

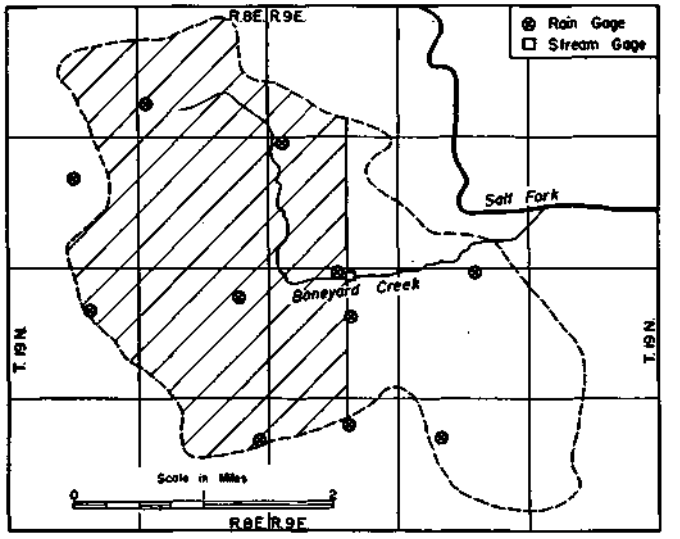

FIG. 3. BONEYARD CREEK RAINGAGE NETWORK, URBANA-CHAMPAIGN, ILL.

only 20 gages could be included in an area of the size and shape of Panther Creek. The question immediately arose as to the comparability of the data; that is, what differences exist in the area-depth curve for a 95-square-mile area when the results are based on a 40-gage network as against a 20-gage network.

Gage density in the following discussion refers to the average area per gage. The 40-gage network corresponds to 2. 4 square miles per gage and the 20-gage network to 4. 75 square miles per gage. To check the effect of gage density, the eight storms of the 1950 thunderstorm season having an areal mean rainfall in excess of 0. 50 inch were analyzed using raingage networks of 40 and 20 gages on the 95-square-mile watershed. Area-depth curves for each storm were determined by planimetering isohyetal maps. The 20-gage network gave the true area-depth relationship. Interpolation was not extended below 10 square miles, since it was felt that the 20-gage networks were not dense enough for this purpose. (There is a tendency to underestimate the mean rainfall considerably for small units of area where gage densities are insufficient to sample small intense cores of rainfall with accuracy.)

Percentage differences summarized in Table I were determined by comparing the 10-, 25-, 50-, 75- and 95-square-mile points on area-depth curves for 20- and 40-gage networks. Although the 20-gage network did not give quite as detailed isohyetal patterns, the variation in the constructed area-depth curves was minor within the limits tested. It was felt, therefore, that the 1948-1949 network of 20 gages per 95 square miles (4. 75 sq. mi. /gage) could be used for analysis with a good degree of confidence in the results.

Since the 20-gage network appeared to give area-depth curves very close to the true curve, it was decided to further investigate the effect of gage density upon the area-depth curve obtained. To do this, area-depth curves obtained from gage densities of 4. 75, 9. 5, and 19. 5 (20, 10, 5 gages) for the 15 heaviest storms during the 1948-1950 period were compared. The 9. 5 and 19. 5 results were expressed as percentage differences from those obtained with the 4. 75 gage density. Table 2 summarizes the results. The results indicated, as would be expected, an increasing error with decreasing gage density, the error being greatest at the smaller units of area. Departures from the true mean were predominately negative, demonstrating the tendency of the sparser networks to miss or underestimate the heavier cores of rainfall. The 5-gage network was not extrapolated below 25 square miles since it corresponds to but one gage per 19. 5 square miles.

Thunderstorm Rainfall. Before proceeding further with the discussion of the area-depth analysis, it would appear desirable to review the nature of thunderstorm rainfall. Byers and Braham (1) have shown as a result of radar-thunderstorm studies in Ohio and Florida that the thunderstorm is normally multicellular in nature. Usually a thunderstorm consists of three or more cells adjacent to each other, each manifesting itself in the surface rainfall pattern. They found that single, isolated thunderstorm cells were comparatively rare, and generally weak when they did occur. The duration of moderate or heavy rain from a single cell of a storm was found to vary from a few minutes to almost an hour depending upon the life of the cell.

The thunderstorm squalls preceding cold fronts, probably the most frequent source of heavy rainfall in the Panther Creek region and much of the Midwest, were found in the present study to be composed most frequently of several squall lines comprising a squall zone rather than a single line of thunderstorms. This leads to the conclusion then that the surface rainfall pattern will be dependent upon several factors including the number, size and longevity of the individual cells affecting the area, and their distribution of showers within the area of interest.

The thunderstorm project found that these cells may vary anywhere from one to more than thirty miles in diameter. Consequently, these factors will be reflected in the area-depth curve. The complexity of the rainfall pattern will tend to increase with area and decrease with time. That is, the number of cores or centers of heavy rainfall associated with the individual cells will tend to increase with area, especially with squall line conditions. The increasing number of cells crossing an area with progressing time will usually tend to make the total storm pattern more uniform due to the overlapping effect. For relatively large basins and short storm durations, the area-depth curve will often reflect a composite effect of several rainfall cores or centers within the area rather than a pattern of high rainfall at one place decreasing progressively outward from the single center.

SOME FACTORS AFFECTING AREA-DEPTH RELATIONSHIPS ON INDIVIDUAL BASINS

The area-depth curve will be influenced by the size and shape of the basin, the orientation of the storm with respect to the basin, topography, duration of storm, and type of storm. The Panther Creek studies have been chiefly concentrated on the summer thunderstorm type of rainfall over this watershed, which is comprised of relatively flat terrain with no distinct topographic features. For this investigation, therefore, three variables, size and shape of basin, general type of storm, and topography, are fixed. The efforts have been concentrated on the effects of storm duration and storm location with respect to the basin.

With respect to storm location, it may be said that a given storm consisting of a single rainfall core or storm center traveling along the minor

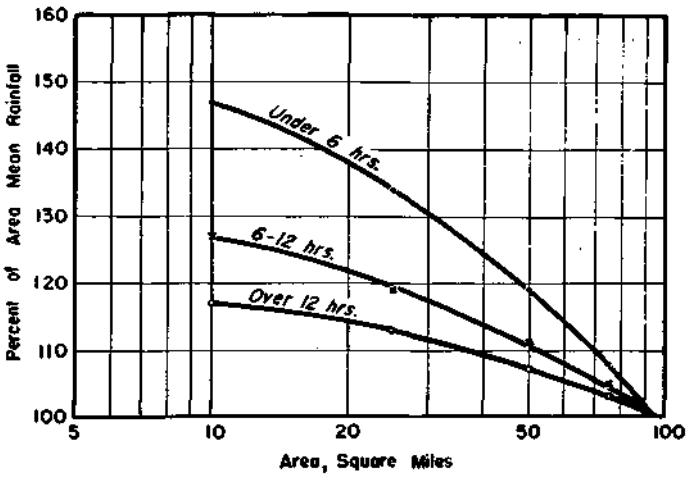

FIG. 4. PERCENT AREA-DEPTH CURVES FOR THREE STORM DURATIONS. 1948-50 DATA.

axis of a rectangular basin, will produce an area-depth curve of greater slope than the same storm having its center coinciding with the major axis of the basin. That is, the range of rainfall values from the lower end to the upper end of the curve will be greater. Similarly, when the storm axis passes near or outside the basin boundary, the slope will be greater than when the storm center passes through or near the basin center.

Table 3 illustrates these effects, using data from the July 16 to 17, 1950, storm, which was the heaviest recorded during the three-year observation period. Three conditions have been illustrated using a 12 x 8. 3 rectangle (100 sq. mi.) superimposed on the storm rainfall pattern. First, the major axis of the rectangle was made to coincide with the storm axis. In the second case, the minor basin axis was made to coincide with the storm core, and third, the rainfall core was placed along the basin boundary parallel to the basin major axis. This was done for the total storm period and for the three-hour period of maximum rainfall within the over-all storm to illustrate the effect of duration as well as location on the area-depth curve. The area-depth values in each case have been expressed on a percentage basis to better illustrate the relative variation. The effect of storm position and duration are readily apparent, the variation being least with the longer duration and with the storm axis passing along the basin major axis. The effect may be greater or smaller than the illustrated example, depending upon the basin characteristics, storm core locations and durations involved.

Area-Depth Analysis, 95-Square-Mile Watershed, 1948-1950. Twenty-eight storms having mean rainfall in excess of 0. 50 inch for the 95-square-mile watershed during the 1948-1950 period were used in the study. Of these, 14 had the axis of the rainfall core passing near the center of the basin, while the remaining 14 passed near the boundary of the basin. As would be expected, the heaviest area rainfalls occurred with those storms having their area of heaviest rainfall near the basin center. Since these are the storm types producing the heaviest rainfall for a given area, they have been analyzed separately. The results should be quite typical of area-depth relationships in heavy rain storms.

Percentage area-depth relationships for these 14 storms have been listed in three classes in Table 4, corresponding to rainfall durations of over 12 hours, 6 to 12 hours, and less than 6 hours. Figure 4 shows mean percentage depth curves for each of the duration classifications. Partial storm periods for several of the heavier storms have been utilized in the analysis, since they comprised unit storms within the over-all storm period representing the passage of squall lines or zones. A further breakdown involving the orientation of storm cores with respect to the basin axis was not possible with the limited data. In these cases, however, it should be a minor factor, since the basin is not of an elongated nature, being roughly equivalent to a 9 x 11 rectangle.

Figure 4 indicates that the slope of the area-depth curve tends to decrease considerably as rainfall duration increases. This tendency is most pronounced when proceeding from the relatively short duration (1-5 hours) to moderate durations (6-12 hours). Variations between the percentage area-depth curves for individual storms became smaller as the rainfall duration increased. For a specific duration, the variations between individual storms were less for large areas than small areas. Considering the nature of thunderstorm rainfall, these indicated tendencies are quite logical. As pointed out earlier, the thunderstorm is multicellular in nature, so that as storm duration increases and the number of individual cells crossing a given area increases, there will be an increasing tendency toward uniform areal rainfall.

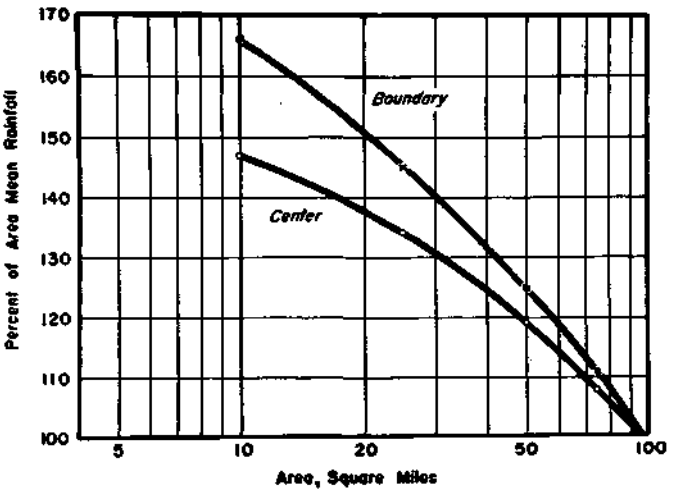

FIG. 5. STORM CENTER LOCATION AND AREA-DEPTH DISTRIBUTION.

Table 5 and Figure 5 show a comparison between 14 storms with storm axis located near the boundary of the 95-square-mile watershed with six storms having their core of heaviest rainfall near the central part of the basin. Comparison could only be made for storms of less than six hours duration, since all 14 boundary storms fell into this classification. As would be expected, the slope of the boundary-storm curve is greater as a rule. With respect to a basin, the rainfall gradient decreases mostly in one direction in the boundary storms. As a result, the mean rainfall for the total area decreases considerably compared to the same storm passing near the basin center. However, the maximum rainfall remains as high or nearly so as when the storm core is well within the watershed boundaries. This, of course, results in a greater slope for the area-depth curve with boundary storms.

It should be mentioned here that the limited data did not permit a thorough analysis of possible effects of the magnitude of storm rainfall on the slope of the area-depth curve. The Weather Bureau study (2) of 38 six-hour partial storm periods found no evidence of.any significant change in slope with increased mean rainfall in these six-hour periods. The limited data in Table 4 point in the same direction. Comparing the three storms of greater than 12-hour duration, no significant differences in percentage values are evident, although mean rainfall varies from 2. 57 to 5. 22 inches. Similarly, for the five storms of 6-12 hours' duration, there appears to be no significant correlation with mean rainfall, although amounts range from 1.14 to 2.77 inches. A similar conclusion may be drawn from examination of the storms of less than six hours' duration. Rainfall duration appears to be more important than total thunderstorm rainfall in determining the slope of the area-depth curve.

The tendency for the area-depth curve to decrease in slope with increasing duration of rainfall is further illustrated in Table 6 and Figure 6, where percentage area-depth relationships for three-hour intervals in the storm of July 17, 1950 are compared with the same values for the total nine-hour storm period and with those for the over-all storm. This storm consisted of two three-hour periods of relatively heavy rainfall separated by a three-hour period of relatively light precipitation. In connection with this table, it is interesting to note that the three-hour period of light rainfall having the greatest slope showed the heaviest rainfall amounts near the edge of the watershed, while the axis of the rainfall core in the two heavy storms passed well within the watershed boundaries.

Comparison of 5. 2-, 95-, and 280-Square-Mile Watersheds. Comparison of area-depth data for the 95-square-mile watershed was made with that collected from the Boneyard watershed of 5. 2 square miles and the 280-square-mile Panther Creek area. Comparison between the three areas was possible only for storms of less than six hours' duration since insufficient data for the Boneyard were available for longer durations. Table 7 and Figure 7 show this comparison for storms whose heaviest rainfall was located near the central part of the watersheds. Table 8 shows a comparison of average percentage area-depth values for storms having their rainfall cores near the watershed boundary with those having cores well within the basin area for each of the three watersheds. Table 9 shows percentage area-depth relationships for the 280-square-mile area for three storms of longer duration with storm cores near the basin center.

From Table 7 and Figure 7, the tendency for storm rainfall variability to increase with increasing basin area is apparent. This variability is illustrated in another manner in Figure 8, where each basin is treated as a unit area and mean percentage area-depth curves constructed for the three basins. In referring to Figure 7, it should be remembered that the average relationships for the 5. 2-square-mile watershed are not strictly representative of the maximum 5-square-mile area relationships in the larger watersheds. With increasing basin area, the number of thunderstorm cells, and consequently the number of intense cores of rainfall, tends to increase. This will result in a trend toward lesser variability in the area-depth curve within the very small areas of heaviest rainfall in the larger watersheds.

The dashed portions of the curves in Figure 7 represent estimated relationships. Since the

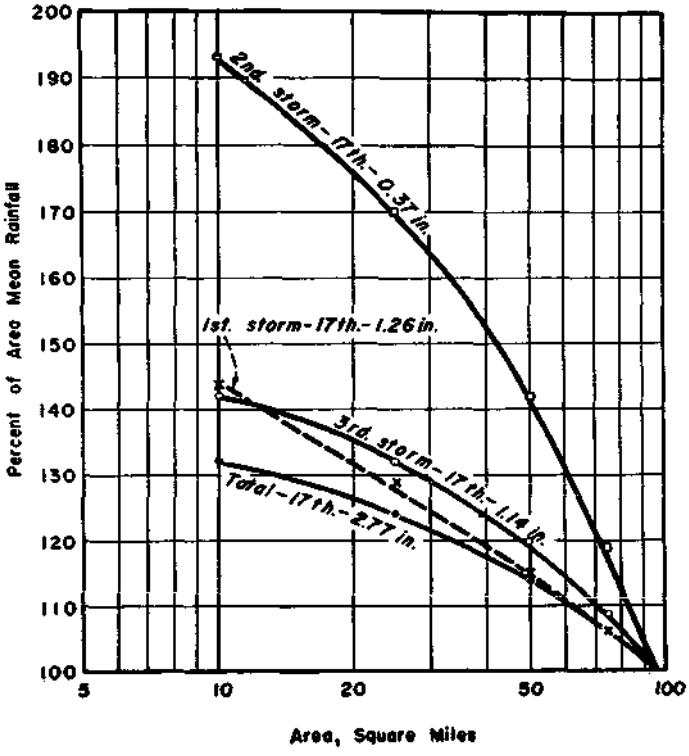

FIG. 6. PERCENT AREA-DEPTH COMPARISONS FOR PARTIAL STORM PERIODS AND TOTAL STORM, JULY 17, 1950.

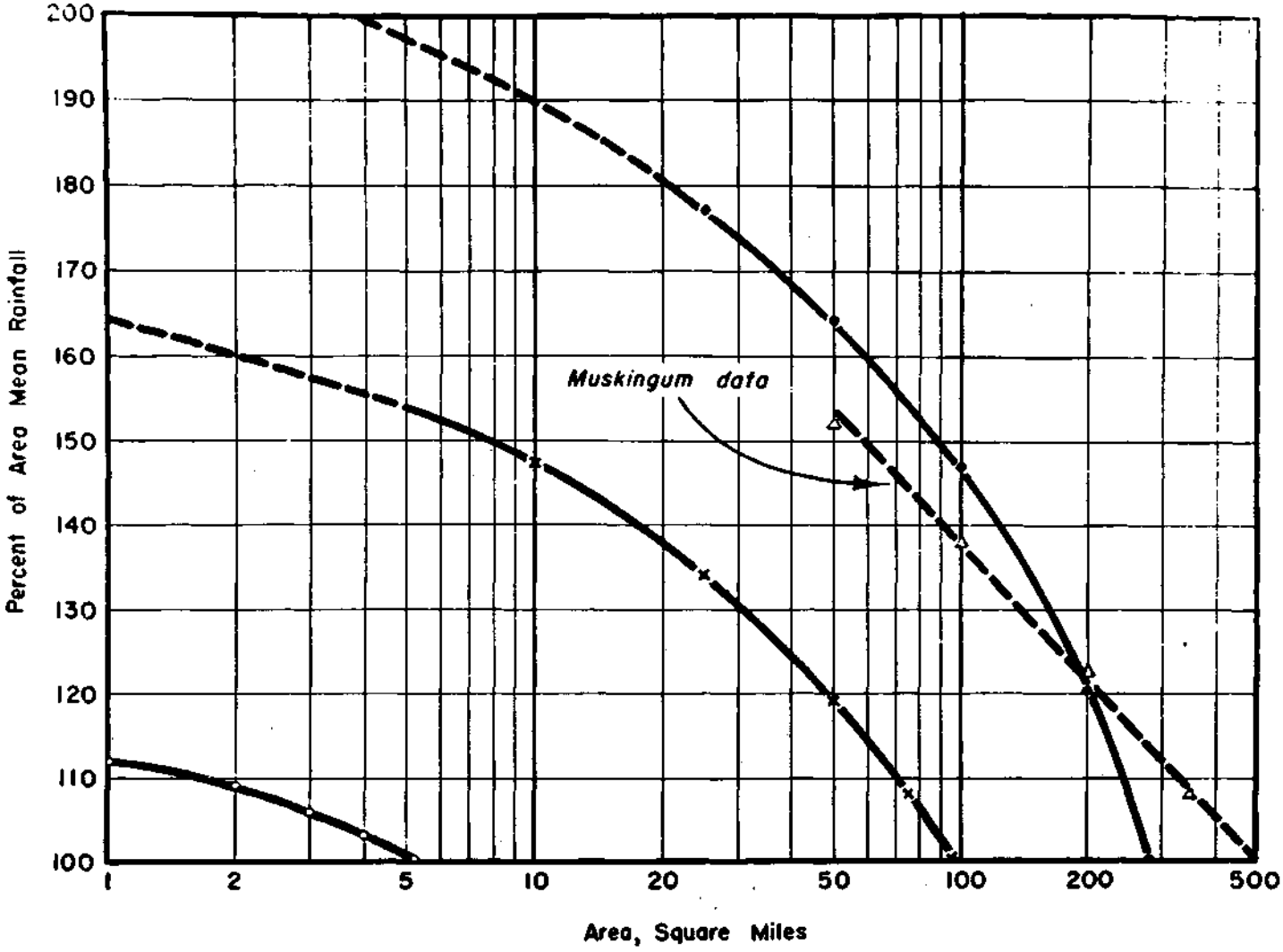

FIG. 7. AREA-DEPTH CURVES FOR THREE NETWORKS IN ILLINOIS. Storm cores near area center. Durations less than 6 hours.

three curves for the individual watersheds are strikingly similar in shape, the curves for the 5.2- and 95-square-mile basins were used as guides in extrapolating the 280-square-mile basin curve. This was done by plotting the necessary portions of the 5.2- and 95-square mile curves at the upper end of the 280-square-mile curve. Similarly, the 5.2-square-mile curve was used as a guide in extrapolating the 95-square-mile curve. The results are presented as an approximation of the actual relationships in the absence of more concrete data. As stated before, applying directly the actual percentage values for a small watershed to the upper end of a curve for a larger watershed would tend to give erroneously high values. As an example, the ratio of the one-square-mile rainfall to the area mean determined for the 95-square-mile basin would be 1.71 by this method, while that obtained by the extrapolation method was 1. 64.

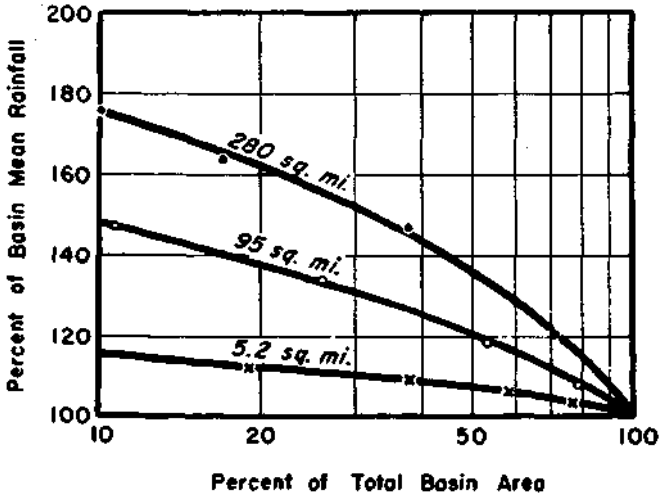

FIG. 8. EFFECT OF NETWORK AREA ON STORM RAINFALL VARIABILITY. Durations less than 6 hours.

The Muskingum data in Figure 7 represents average values obtained from an analysis of 38 storms on the Muskingum Basin in Ohio by the U. S. Weather Bureau Hydrometeorological Section (2). Figure 9 expresses the area-depth data for the 5.2-, 95-, and 280-square-mile basins as a percentage of the maximum one-square-mile

mean rainfall. This type of curve is sometimes used for design purposes. The 95- and 280-square-mile curves again are presented as close approximations, since the value of the one-square-mile mean may not be strictly accurate.

Table 8 indicates that area-depth curves for boundary storms ordinarily show greater variation with decreasing area than do centralized storms in all three watersheds. This effect minimizes when proceeding from small units of area to large units in a given watershed. The effect of the small intense cores of rainfall decreases as greater area is encompassed on the area-depth curve.

Table 9 gives some limited percentage area-depth data for longer duration storms in the 280-square-mile basin. Comparison with Table 7 values for storms under six hours' duration again indicates decreasing variability with increasing rainfall duration.

GAGE DENSITY-MEAN RAINFALL RELATIONSHIPS

It is important to know the reliability of mean rainfall values obtained from raingage networks of varying density which may be used for determination of basin rainfall-runoff relationships. This is especially true for small watersheds with thunderstorm rainfall where only limited information is available, since raingage networks ordinarily employed do not provide sufficient data for such an investigation. Except for those provided by Light (2), Langbein (3), and Linsley (4), very few data are available on the errors involved in the computation of areal mean rainfall.

Although the data collected from the concentrated networks used in this study are too limited to establish definite quantitative relationships, it is believed that they do show the general magni-

FIG. 9. MEAN PERCENTAGE AREA-DEPTH CURVES.

tude of error associated with different gage densities for the size and type of watersheds investigated. The investigation is being continued to gather further information.

Data from the 95-square-mile basin described in the section on area-depth relationships and shown in Figures 1-2 were used in the study. Observations from 20 gages on this experimental area were available for May-September 1948-1949 and from 40 gages for the same period in 1950.

Analysis of Data. It was assumed that the true mean rainfall was determined by the network of 20 gages on the 95-square-mile watershed. This corresponds to an average density of 4. 75 square miles per gage. Although the assumption necessarily involved some error, it was believed that it would be of small magnitude. As a partial check on the assumption, a comparison of results from 40- and 20-gage networks on the 95-square-mile watershed for 1950 was made. This comparison is summarized in Table 10, where it is seen that both mean differences and maximum differences obtained from the two networks were of relatively small magnitude.

Mean Error vs. Gage Density. The reliability of mean rainfall as determined from networks of 10, 5, 3, and 1 gages on the 9-square-mile watershed was investigated next. These networks correspond to average densities of 9. 5, 19. 5, 32, and 95 square miles per gage. Stations were chosen to give as uniform a network as possible in each case. Where only one gage was used, it was the most centrally located one. Mean rainfall was classified into four intervals, .01-.20, .21-.50, .51-1.00, and 1.01-3.00 inches, to determine the effect of storm magnitude upon the error involved with each raingage network. The error in each case was determined from the difference between the 20-gage mean rainfall and that obtained from the network in question.

The results are shown in Table 11 and Figures 10 and 11, where the mean error for each mean rainfall classification and each raingage network has been expressed in both inches of rainfall and as a percentage of the true mean or 20-gage average rainfall. It can be seen that while the absolute magnitude of the error (inches) increases with increased mean rainfall, it is proportionally smaller with the heavier storms. Based on an average for a number of storms, the mean error is relatively small, except for the heavier storms with the single gage. For general climatic purposes, therefore, it would appear that concentrated networks, such as employed in the three-year period studied are not justifiable.

Frequency Distribution of Errors. To further investigate the occurrence of errors in the determination of mean rainfall, frequency distributions of these errors for the different gage densities and mean rainfall classifications used in Table 11 were computed from the 1948-1950 data. The results are summarized in Table 12. Data were too limited to justify a more detailed analysis. It is apparent from the results that the permissible error should determine the gage density employed in any situation. Much detail is lost in isohyetal patterns as the gage density is decreased, due to the small areal extent of thunderstorm cells. Figure 12, showing isohyetal patterns drawn for the July 16-17, 1950 storm using gage densities of 2. 4, 4. 75, 9. 5, and 19. 5 square miles

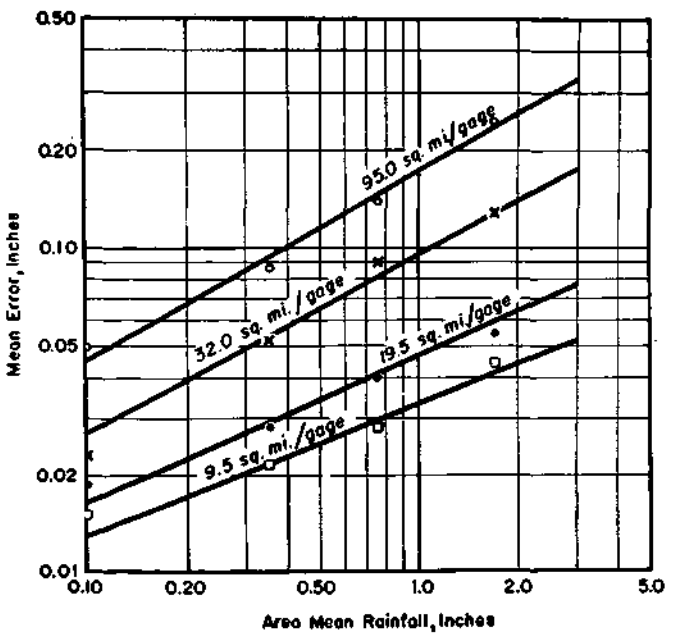

FIG. 10. EFFECT OF GAGE DENSITY AND MEAN STORM RAINFALL ON MEAN ERROR. 95-sq. -mi. area, 1948-50. Assuming 4. 75 sq. mi. /gage gave true area mean.

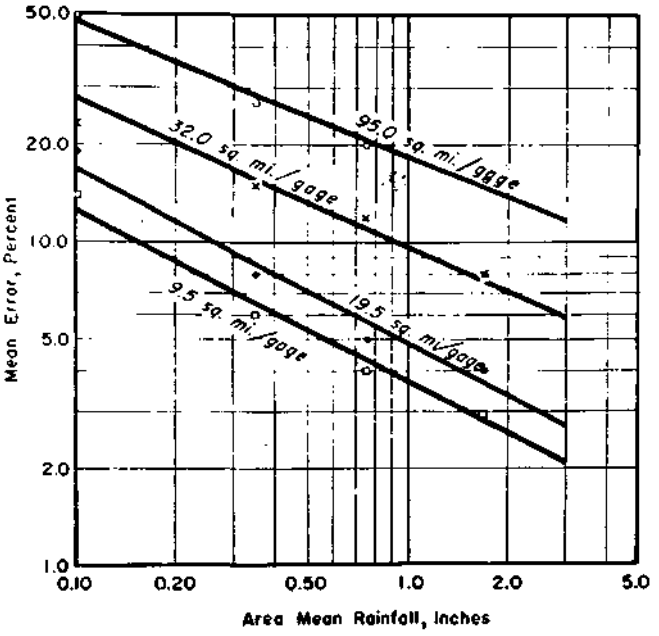

FIG. 11. EFFECT OF GAGE DENSITY ON PERCENT ERROR FOR VARIOUS STORM RAINFALLS. 95-sq.-mi. area. 1948-50. Assuming 4. 75 sq. mi. /gage gave true mean area.

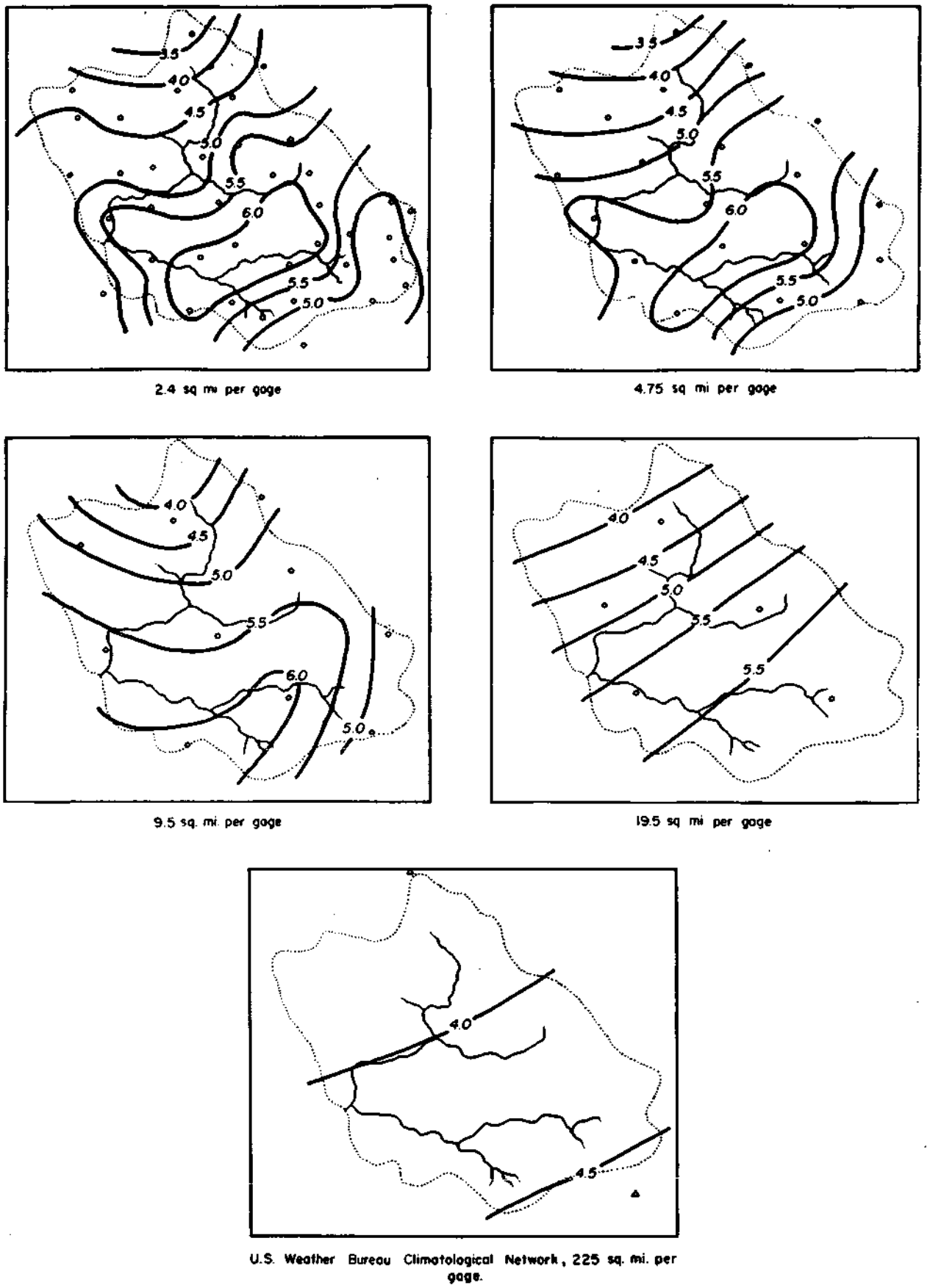

FIG. 12. EFFECT OF GAGE DENSITY ON ISOHYETAL PATTERN.
Storm of July 16-17, 1950.

per gage, illustrates this point. The gage density employed, therefore, will also depend upon the detail desired in the isohyetal pattern.

Error vs. Gage Density, Monthly and Seasonal Basis. Table 13 shows a summary of the errors for different gage densities on a monthly and seasonal basis. The data -indicate that, for monthly rainfall, one gage per 95 square miles gives a mean error less than 10 per cent most of the time, especially with the heavier areal rainfalls. Since the greatest errors would ordinarily occur during the thunderstorm season, it appears that a network of one gage per 100 square miles should be sufficient for the determination of monthly or seasonal mean rainfall for most purposes. Monthly and seasonal accuracy improves but slightly with increasing gage density. The errors are predominately negative, illustrating the tendency of the less dense networks to miss or underestimate areas of most intense rainfall. This, of course, is also true for storm rainfall.

STORM TYPE AND RESULTANT RAINFALL

Areal Mean Rainfall vs. Storm Type. The frequency distribution of areal mean rainfall by storm types over the 95-square-mile basin for the thunderstorm seasons 1948-1950 was investigated. Storm precipitation was divided into five classes for this study. These classes included rainfall occurring with cold fronts, pre-cold frontal squall lines, warm fronts or warm air overrunning, warm air mass instability, and cold air mass instability.

The storm type associated with each rainfall occurrence was determined from U. S. Weather Bureau daily synoptic maps. For the purpose of this investigation: (1) Cold front precipitation was defined as that occurring from 100 miles in advance of the front until ending of the rainfall with the frontal passage. (2) Pre-cold frontal squall lines included those occurring in the warm air mass from approximately 100-300 miles in advance of a cold front and were considered to be indirectly associated with cold fronts. (3) The warm front type rainfall included that associated with the approach and passage of warm fronts or warm air overrunning from stationary fronts located to the south. (4) Warm air mass instability rainfall was defined as that occurring in warm air masses in the absence of fronts and included thermal convection and nocturnal thundershowers. (5) Cold air mass instability showers included those occurring in the cold air mass well after the passage of the cold front, usually associated with the passage of a trough aloft.

All storms resulting in an areal mean rainfall of 0. 01 inch or more were included in the analysis. In cases where a warm front passage was followed by a cold front passage within a few hours, the rainfall associated with each system was determined from a study of the synoptic maps and the recording gage records. A similar procedure was followed with fronts which became stationary over southern Illinois after passing through the experimental area as cold fronts.

In Table 14, a comparison between storm type and areal mean rainfall has been summarized. As should be expected in the region in which the experimental area lies, precipitation was most frequently associated with cold fronts during the thunderstorm season. Similarly, the largest proportion of the areal mean rainfall was either directly or indirectly associated with cold fronts. During the three-year period, cold fronts and pre-cold frontal squall lines accounted for 50 percent of the total storms and 66 percent of the total rainfall.

Perhaps more significant to the hydrologist and meteorologist is the frequency distribution of the heavier areal mean rainfalls by storm type. Table 15 shows a comparison between storm type and areal mean rainfalls of 0. 50 inch or more. It can be seen that cold frontal and pre-cold frontal squall lines were again dominant, accounting for 80 percent of the storm rainfalls of 1. 00 inch or more and 71 percent of those equaling or exceeding 0. 50 inch. It is interesting to note that no warm air mass type, which includes heat convection thunderstorms, gave an areal mean rainfall of 1. 00 inch or more. Although the heat convection thunderstorms may produce heavy rainfall intensities, they normally consist of scattered or isolated storm cells of small areal extent and short duration. Opportunities for heavy areal rainfall on a 95-square-mile watershed are considerably greater with the multicellular thunderstorm lines or zones associated with the approach and passage of cold fronts, where rainfall may continue for several hours.

Rainfall Intensity vs. Storm Type. A study was made of the excessive rainfall rates recorded on the 95-square-mile watershed during May-September, 1948-1950. Only data from recording gages could be used for this purpose. During the 1948-1949 seasons, 8 recording gages were included in the 20-gage basin network. The number of recording gages was increased to 24 during 1950.

Excessive rainfall rates were determined from the following U. S. Weather Bureau formula for short-period, high intensity storms:

$$R = 0.01\ (t + 20),$$

where R is rainfall in inches and t is time in minutes.

Excessive rates were determined for 30-minute, 1-hour, and 2-hour storm periods. Since weekly recording charts were used on the gages, analysis of excessive rates for smaller units of time was not practical. Excessive rates for 30 minutes, 1 hour, and 2 hours correspond to 0. 50

inch, 0.80 inch, and 1.40 inches respectively.

During the three thunderstorm seasons, there was a total of 25 storms in which excessive 30-minute rates were recorded by one or more of the recording gages (Table 16). Similarly, there were 19 storms in which excessive 1-hour rates occurred, and 9 storms with excessive 2-hour rates.

Storms associated either directly or indirectly with cold fronts were the chief source of heavy intensities. Cold fronts and pre-cold frontal squall lines accounted for 75 percent of the storms with excessive 30-minute rates, 84 percent of those with excessive 1-hour rates, and 89 percent of the storms with excessive 2-hour rates. The maximum intensities recorded by an individual station occurred with a pre-cold frontal squall line on July 16, 1950. A 30-minute total of 1. 46 inches was recorded by one station, while another recorded 1-hour and 2-hour totals of 2. 25 inches and 2. 72 inches respectively. This storm was also the source of the most widespread occurrence of excessive rates. Table 17 shows the occurrence of 30-minute amounts exceeding 1. 00 inch. Again, the cold front systems were dominant, accounting for 7 out of 8 storms with one or more stations recording over 1. 00 inch in 30 minutes. Thus, storms associated either directly or indirectly with cold fronts were the most frequent source of rainfall, the source of the heaviest mean storm rainfalls, and the source of the heaviest rates of rainfall in the 95-square-mile experimental area.

RADAR STUDIES

The very close correspondence between the storm pattern shown by the radar and the rainfall pattern occurring on the ground has been established; but the possible application of this relationship in engineering meteorology has not been explored. Prominent studies were carried out by the Massachusetts Institute of Technology Weather Radar Research Project, whose report of December 1946 (5) summarized the results to date.

The U. S. Signal Corps has played a leading role in sponsoring the M.I. T. work as well as carrying on a number of separate studies (6, 7, 8). The British, through Ryde (9), and Marshall and others of the Canadian Army Operational Research Group (10) have contributed much to the theoretical knowledge of the relation of radar echo to rainfall and other meteorological parameters.

In the application of radar for storm detection, the Army-Navy-National Advisory Committee on Aeronautics - Weather Bureau Thunderstorm Project explored the structure and dynamics of the thunderstorm in great detail. In a preliminary study the possible use of radar in estimating the amount of rainfall over a small area (11) was established by Byers et al. The Ail-Weather Flying Division of the Air Force recognized the possible uses of radar in aviation meteorology and Atlas combined the theoretical and empirical weather radar equations to form the basis for a simplified Radar Rain Intensity Computer (12).

However, none of the above-mentioned projects have provided sufficient data and conclusions to establish radar as a dependable quantitative instrument.

PRINCIPLE OF RADAR

The radar set emits a short, intense pulse of energy which may be focused into a narrow beam and which travels at the speed of light. If the beam strikes an object, such as an airplane or a rainstorm, a small portion of the energy is reflected and returns as an "echo" to the point of transmission. It is then amplified and presented on a cathode ray tube. The range and bearing of the object are readily determined. The beam generally travels along a "line-of-sight," hence the radar cannot detect distant subjects that are near the earth's surface.

Theory. Studies in this field indicate that the radar echoes from precipitation are the result of scattering of radio energy by water drops falling through the atmosphere or suspended by strong vertical currents. The theoretical expression that has been developed (13) indicates that the energy (power) received from precipitation (reflected back to the radar antenna),

$$P_r = C\, h\, P_t \frac{N a^6}{R^2}, \qquad (1)$$

where P_r = received power

C = constant for the equipment used

h = radar pulse width (duration, expressed as a distance)

P_t = peak pulse transmitted power

N = number of raindrops per unit volume

a^6 = mean sixth power of the radii of the rain drops

R = square of the distance to the object

or

$$P_r = K_1 \frac{N a^6}{R^2},$$

where K_1 absorbs a number of the constants.

From data collected by Laws and Parsons (14) which indicate a relationship between raindrop size and intensity of rainfall, R. Wexler (15) has

concluded that,

$$\text{Log } N a^6 = 1.441 \text{ Log } I - 17.302, \qquad \text{(II)}$$

where I represents the rainfall intensity expressed in mm. /hour; hence

$$P_r = K_2 \frac{I^{1.441}}{R^2} . \qquad \text{(III)}$$

The problem in using radar for rainfall intensity measurement therefore appears to center around determining the power received (P_r), since that is a function of the intensity of the rainfall.

Radar Storm Presentation. Figure 13a represents a hypothetical storm of 5 miles depth, of which the nearest edge is 15 miles east of the radar. The contours represent lines of equal rain intensity, the core of heavy rain being the innermost area. When the radar antenna is directed along axis AB, Figure 13b represents the hypothetical received-power curve, corrected for range and attenuation. The "A" scope, a cathode-ray tube presentation used in many radars, portrays the observed data in a similar form. However, the receiver sensitivity is normally maintained at a high level so that light rain may be observed. As a result the amplitude of the received power curve exceeds the capacity of the receiver circuits, distorting the signal so that moderate rain intensities and cores of heavy rain cannot be distinguished.

The portion of the received-power curve the radar operator observes on the "A" scope is shown in Figure 13c. At maximum receiver sensitivity only the base of the received-power waveform is presented. This represents the area of light rain but the heavier rainfall drives the circuits to saturation, thus flattening the top of the received-power curve. When the receiver sensitivity is reduced, greater received power is necessary to reach the threshold of visibility. It is necessary for the rain intensity to be greater to produce a detectable signal. Thus the area of medium rainfall is presented. The receiver sensitivity may be reduced until only the received-power from the core of heaviest rain is perceptible. The received-power that will cause a barely-perceptible image on the scope is readily measurable.

A different type of presentation is obtained with the PPI (plan position indicator) scope. As the rotating antenna scans all the area around the radar, the PPI presents an image of the storm as if it were laid out on polar coordinates. The area of rain glows while the rest of the face of the scope is dark. Thus the location and areal extent of the storm is readily observed. Figure 14 shows such a view.

The outline of the image at different receiver-sensitivity levels should correspond to a rainfall intensity contour. If the image on the PPI is recorded at several receiver-sensitivity levels, superimposing the areas enables construction of radar-rain intensity contours that should coincide with actual rain intensity contours.

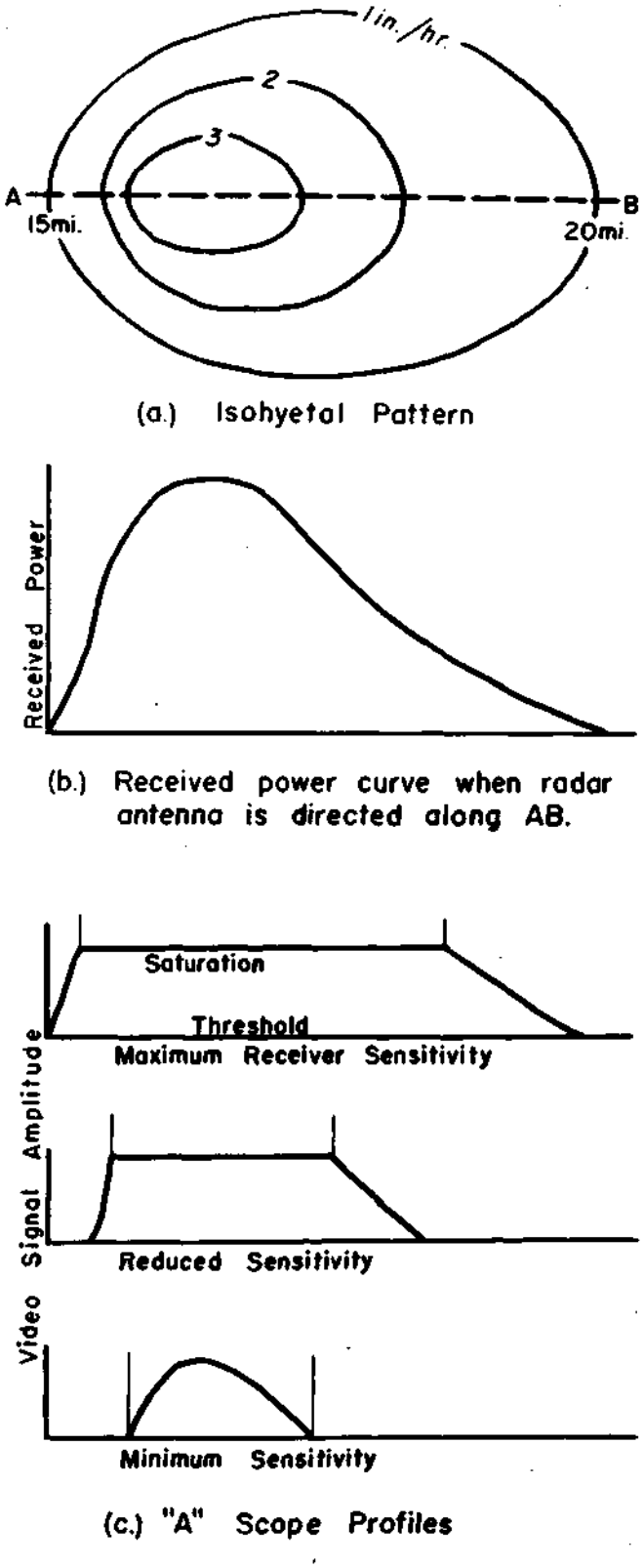

FIG. 13. RECEIVED POWER PROFILES.

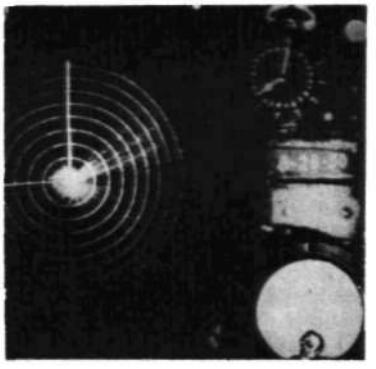

FIG. 14. SCOPE AND DATA OF AUGUST 28, 1950, 1501 C. D. T.

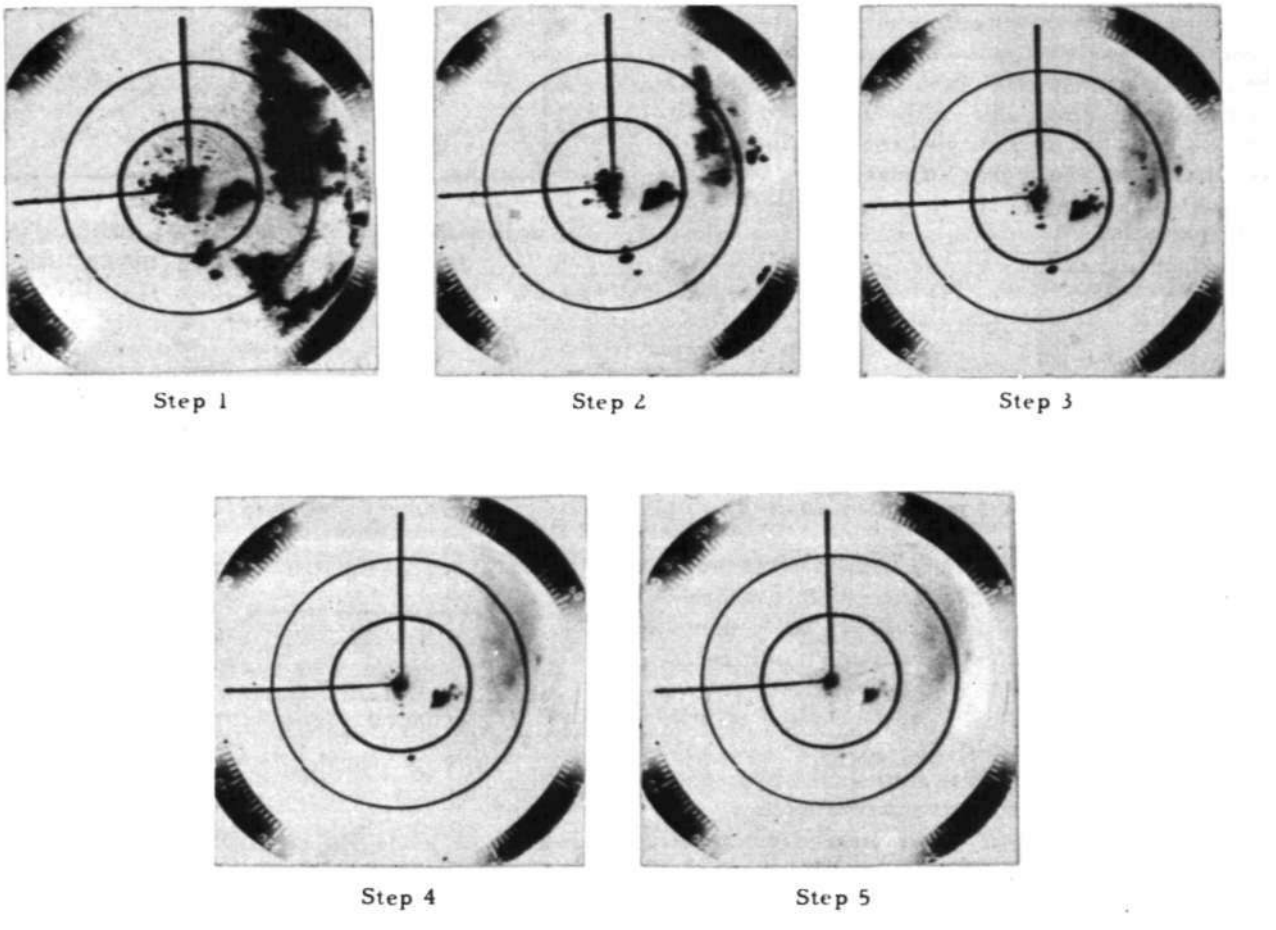

FIG. 15. RADAR RAIN INTENSITY CONTOURS AS PRESENTED ON THE PPI WITH THE AUTOMATIC SENSITIVITY CONTROL CIRCUIT. There is a 10-second interval between each photo.

Methods Available. Two methods of varying the receiver sensitivity were used by the All-Weather Flying Division (12, 16).

In one method the receiver-sensitivity control was calibrated in terms of echo power necessary for threshold of visibility of the PPI. The operator manually changed the sensitivity, photographed the PPI image on each setting, and recorded the receiver sensitivity setting for each picture. A picture taken at maximum sensitivity showed the outline of the entire storm while at minimum sensitivity the picture showed the location of the cores of heavy rain.

The second method used by the All-Weather group, the video-inversion method, presents the storm structure as alternate bands of bright and dark areas. The light rain around the outside of the storm (area between contours 1 and 2 in Figure 13a) would appear bright. Heavier rain (contours 2 to 3) would show as a dark area while the core of the heaviest rain (inside contour 3) would appear as a bright area for the center of the storm. This method necessitates considerable additional circuitry.

Neither method seemed to fill all the immediate requirements. The video-inversion method requires a large number of additional tubes and associated circuits. Manual recording of sensitivity settings appeared laborious when several pictures were taken every minute. Since an automatic system of film recording was already in use, an automatic system of receiver sensitivity control operating in synchronism with the camera was developed.

METHOD USED

The radar set in the Pfister Building at El Paso is located 15 miles east of the Farm Creek raingage network (Figure 16). An AN/APS-15 3-cm. radar was used for the study. This unit is calibrated in nautical miles. Its peak power output averages 35 kw.

For this study receiver sensitivity was varied by predetermined steps and the storm pattern on the PPI scope was recorded on 16 mm. moving picture film. An automatic photographic recording and sensitivity stepping circuit was devised. Known values of receiver power were put into the equipment to calibrate the circuit. A series of negatives exposed on August 30, 1950 (Figure 15) show the effect of stepwise receiver sensitivity changes on the image on the PPI scope. The entire series was taken in a period of one minute.

The first picture is on step No. 1. The range marking circles are at intervals of 10 nautical miles. "Ground clutter" due to reflections from buildings extends out to about eight miles. The main area of the rain is the black portion to the northeast. A small area extends from five to ten miles due east and four showers are clustered about 10 miles to the south. In the second picture the sensitivity is reduced to step No. 2. Note how the areas of the rainfall images are reduced. The areas of light rain become imperceptible. Each successive step reduces the area of rain that is visible. On step No. 4 the core of only one of the four showers to the south is visible. On step No. 5 the core of heavy rain in the shower eight miles east is the only rain visible.

All rainfall detected on the radar scope during June through September 1950 was recorded on film. The equipment was kept in readiness for operation 24 hours per day, and round-the-clock operators were on hand whenever synoptic conditions indicated the possibility of precipitation. Figure 14 is a photograph showing a heavy rain near Galesburg, Illinois, 80 miles from the radar. For observing summer thunderstorm rainfall, the equipment used seemed to have an effective range of approximately 75 miles. To the right of the scope in this photo may be seen the date card, 24-hour watch used to record time of observation, the antenna tilt indicator, and the step-position indicator light signals.

Rainfall Measurements. To get reliable rainfall data outside the zone of ground clutter, a network of weighing-bucket raingages was placed in service in July 1950 in the vicinity of Washington, Illinois. The network of 31 gages covers the watershed area of Farm Creek (a tributary of the Illinois) and some adjacent area above East Peoria. The gages are generally spaced about 1 1/2 miles apart (see Figure 16). Collectors of 12.648-inch diameter were used instead of the standard 8-inch units. This expanded the sensitivity of the gages 2 1/2 times. The standard drum clock was geared for one drum revolution in a six-hour period. Thus, 5-minute rainfall amounts were easily determined, and one-minute rates of fall were computed with fair accuracy. A laboratory check is being

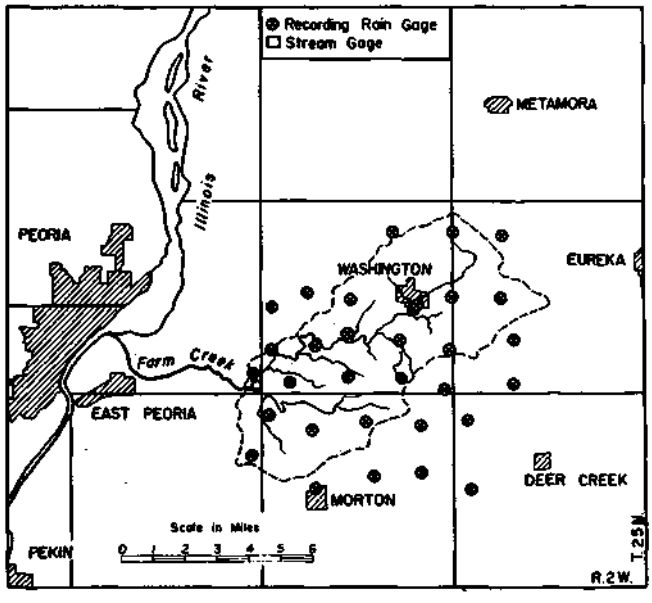

FIG. 16. FARM CREEK RAINGAGE NETWORK, 1950.

conducted to check on lag in the operation of the gages.

Rain fell on 18 days of the 74-day period of operation of the Farm Creek network. On 10 of these days the average amount for the network was less than 0. 10 inch. On the remaining 8 days of rain, the daily totals were as follows: 0. 12, 0.25, 0.31, 0.61, 0.75, 1.33, 1.47, and 2. 54 inches. Widespread shower activity which produced rainfall between the network and the radar set occurred on several days. This introduced an attenuation effect such that only two of the rainstorms could be used in the analysis described in this paper. On several occasions the radar set was not functioning properly and data collected then were eliminated. The data from rainfalls of September 19, 20, and 21 were usable.

There were no cases of rainfall over the Farm Creek network that the radar did not detect and record. On a number of the light rains only a portion of the network received rainfall.

ANALYSIS OF DATA

The data from the raingage network were compiled into form readily available for any type of analysis required. Mean five-minute totals, the maximum rate during each five-minute period, and one-minute rates were tabulated and plotted for selected cases. Isohyetal maps were drawn for five-minute and frequently for one-minute periods of precipitation over the network.

The radar data were transcribed from the 16 mm. film onto a 11 x 17 inch base map by projecting the photograph through a mirror system and a glass-topped copy table. The total area covered during each one- and five-minute period for each different receiver sensitivity setting was drawn. These maps were termed "radar echo contour maps." Figure 17 shows a one-minute radar echo contour map and the corresponding precipitation map. Discrepancies between the two patterns can be attributed to (1) the failure of the radar to detect the entire depth of the storm due to attenuation, (2) time lag due to time of fall from the elevation where the radar detects the raindrops, to the earth, (3) lateral drift of the raindrops in falling, and (4) evaporation of the raindrops while falling. Thus, the areal extent of the precipitation as observed by radar correlates very well with the measured rainfall pattern.

Atlas (16) found that there was a significant correlation between the intense rainfall cores as observed in the lower 5 000 feet of the atmosphere and that measured on the ground below. His best correlation resulted when the surface rainfall was measured at the core of the corresponding precipitation pattern as the average rate over a five-minute interval immediately after the radar observation.

To compensate for the fall time and drift of raindrops from the average height of 2000-3000 feet observed by the radar, successive one-minute maps of radar contours and surface rainfall were used. The one-minute rainfall rates were determined from the slope of the curve on the raingage chart. With the sensitive raingages, it was not difficult to observe rainfall amounts as small as . 005 inch with a time resolution of one minute. Every change of slope, either large or small was considered valid and used in the evaluation.*

The direction and amount of drift were determined from the movement of the radar cores for

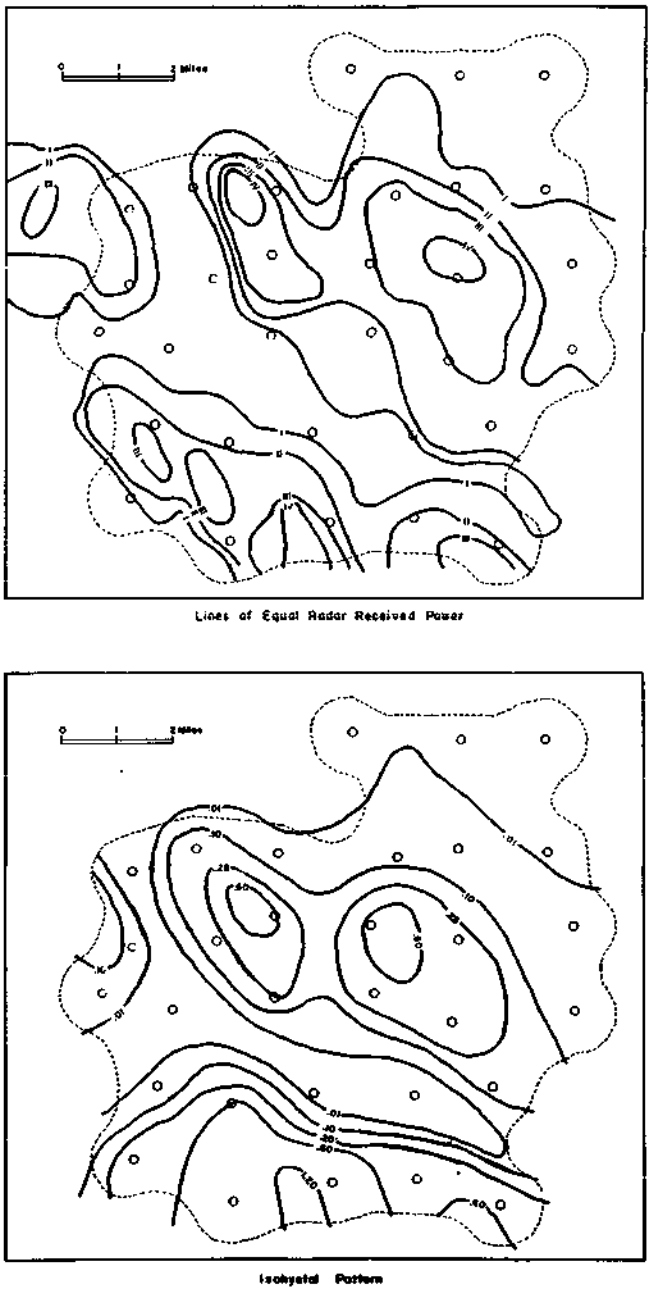

FIG. 17. STORM PATTERN AS SEEN BY RADAR, AND BY RAINGAGE NETWORK. One-minute period. O denotes raingage.

*In most cases, very minor irregularities did not have to be considered since fairly consistent rates persisted for at least 2 to 3 minutes.

several consecutive minutes. The fall time of the raindrops was approximated by comparing a chosen one-minute radar profile along an appropriate radial from the radar station with consecutive one-minute surface rainfall profiles along the same radial, after applying a drift correction to the surface rainfall pattern.

The successive one-minute rainfall profiles were compared with the radar profile until a matching of peaks for location was obtained (Figure 18). Only those cases where the indicated time lag was less than five minutes with drift not greater than one and one half miles were used in the analysis. Cases involving intervening rain and core centers moving off the network were excluded. Where the operators' log showed the possibility of instrumental error or other observational inconsistencies, the data were discarded. Examples of very light shower activity were not considered. When more than one core of rainfall existed, it was often found that the time lag and/or drift varied for each cell. Since the development stage of adjacent cells may vary considerably, this should be expected.

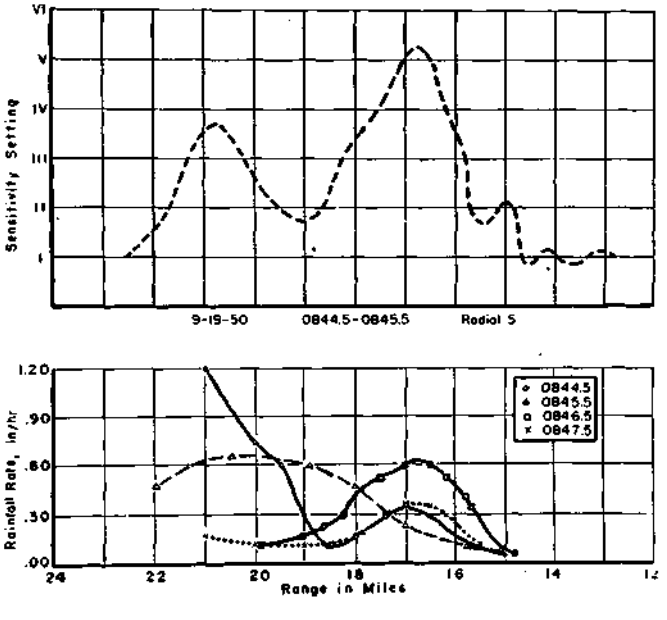

FIG. 18. PROFILES OF RADAR RECEIVED POWER AND RAINFALL INTENSITIES.

Table 18 summarizes the data available. For comparison with published measurements, a function of the received power was used for correlation. Values of $\frac{P_r R^2}{P_t}$ were plotted against the surface rainfall intensities, I_s, in Figure 19. A curve was fitted to the median values of the groups of values.

DISCUSSION

At rainfall rates below 0. 7 inch per hour there is good agreement between the observations gathered in this study and those of Atlas. For higher rainfall rates, there are significant differences in returned signal strength. The Illinois data fail-to indicate the expected exponential relation between rainfall intensities and received power.

Previous studies have indicated that the received power from rainstorms should closely follow the Rayleigh scattering effect. The best available information on drop size (17) would indicate that received power should be exponentially related to rainfall intensity. These drop size measurements were made at the ground surface, however, and the high received-power values at higher rainfall rates may indicate that large drops are present in higher concentrations at the elevations observed by the radar.

The scatter of actual measured rainfall rates (by raingage) shown in Figure 19 was further analyzed to see whether the departures from the curve were such as to indicate any significant lack of correlation with signal strength and range measurements. To do this, the mean rainfall departures from the values indicated by the curve were compared with the errors found under various raingage densities.

The dashed lines in Figure 20 show the mean error (variation from the true mean) associated with mean storm rainfall calculations when raingage networks of various density were employed on a 95-square-mile basin (Figure 11). The solid line represents the mean variation associated with radar determinations of point rainfall intensities. The plotted points are mean values obtained from data for each of the five steps used in determining the Illinois curve of Figure 19. These mean values were calculated from the following equation:

$$V = \frac{100}{N} \sum \frac{D}{R},$$

where V = mean variation, D = deviation of raingage rainfall intensity from the experimental curve value, R = raingage rainfall intensity, N = number of observations.

Despite the limitations of the equipment used, the radar appeared capable of determining point rainfall intensities as accurately as a raingage network of one gage per 100 square miles measured the mean areal rainfall.

Experience gained in this study indicated that the radar was equivalent to gage networks having about one gage per three square miles for determining the areal extent of rainfall. As further work is done, it is expected that increasingly close correlations between radar observations and rainfall intensities will be obtained.

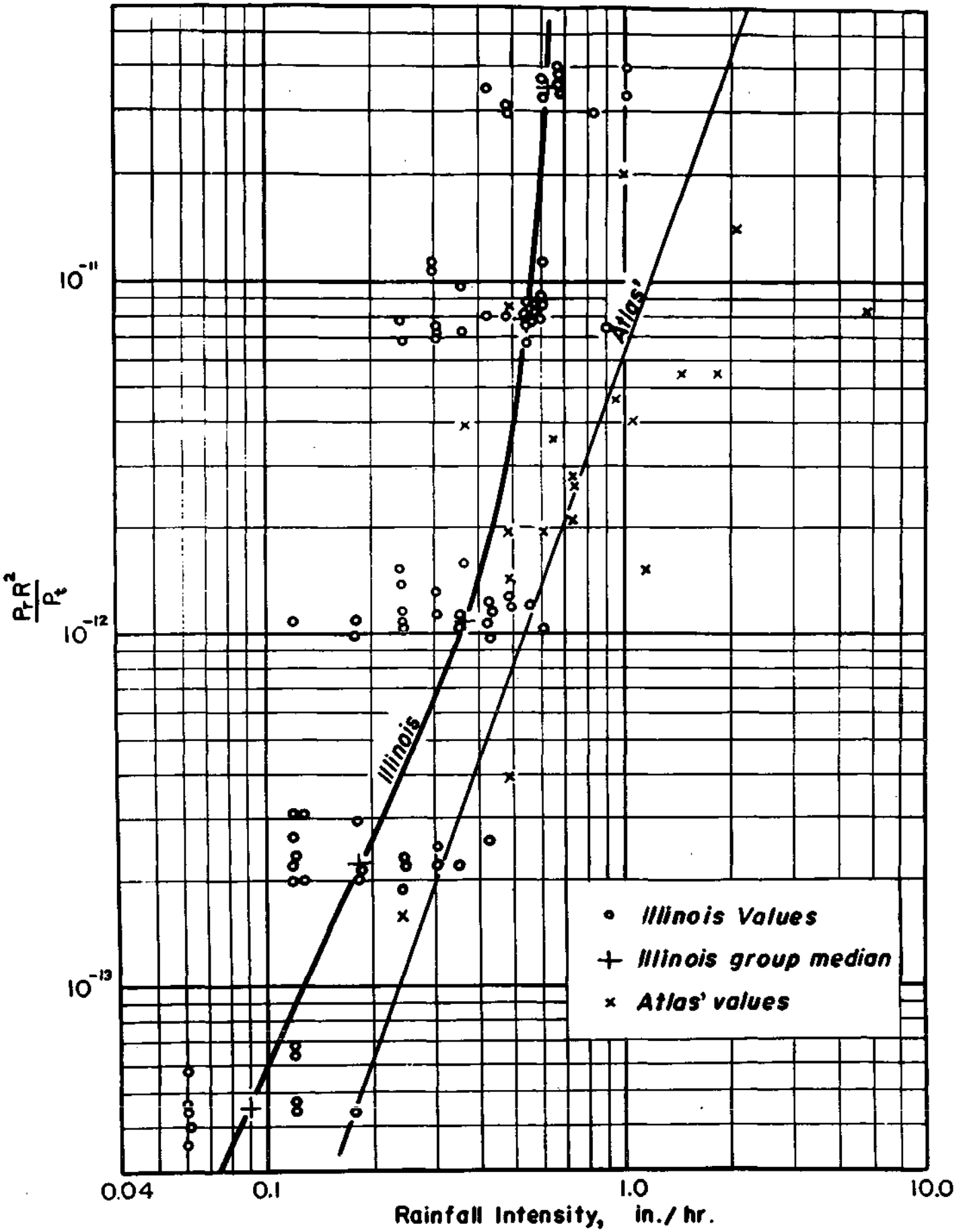

FIG. 19. RECEIVED POWER AND RAINFALL INTENSITY.

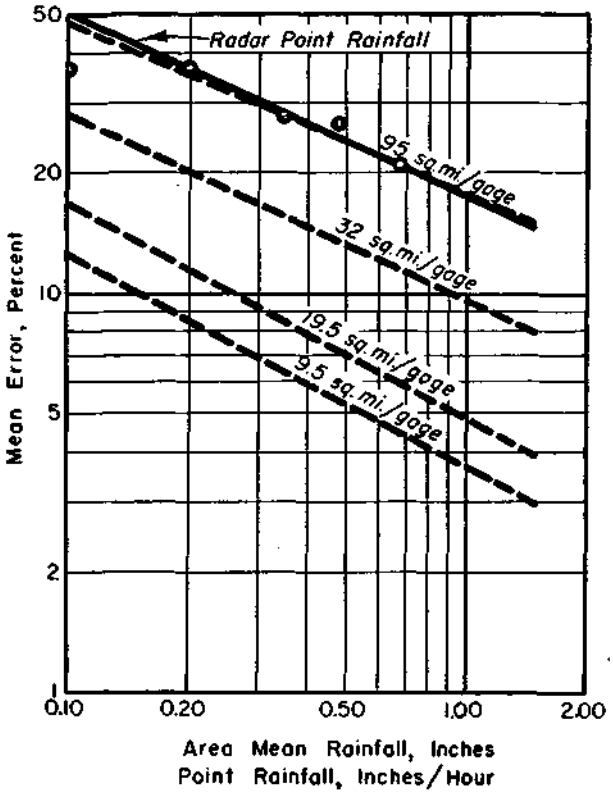

FIG. 20. COMPARISON OF MEAN OBSERVATIONAL ERRORS, AREA MEAN RAINFALL FROM RAINGAGE NETWORKS VS. POINT RAINFALL INTENSITIES FROM RADAR OBSERVATIONS.

Utility of Radar. During the summer of 1950, regular radar-rainfall reports were provided to industry, agriculture, and the public through a local radio station. It is planned to expand this service in 1951 to include quantitative data. The U. S. Weather Bureau put the radar observations on the teletype to augment its information. In highway construction in central Illinois it was found that the precise rainfall location data often enabled extension of operation beyond the usual periods of pouring concrete. Special short range rainfall forecasts were made for the operations of Pfister Hybrid Corn Company, for the University of Illinois commencement exercises, and for the 1949 and 1950 Illinois State Fairs.

Radar can depict precipitation patterns associated with flash floods, large floods, tornadoes, hurricanes, frontal weather, and freezing rain in winter. It will doubtless be used to study drop size and its effect on erosion. It should prove useful in irrigation works, and in controlling water supply reservoirs and hydroelectric plants.

Within the next few years, radar will provide the answers to the area-depth questions that engineers ask.

ACKNOWLEDGEMENT

These studies owe much to the interest, encouragement, and material assistance of Lester Pfister, President of the Pfister Hybrid Corn Company, El Paso, Illinois.

Many staff members of the Illinois State Water Survey have contributed to this study. The radar work was begun under the initiative of Dr. A. M. Buswell, Chief, and the entire study has been carried forward with his strong encouragement. Mr. W. J. Roberts, Associate Engineer, procured the radar and directed its assembly. Mr. Douglas Jones, Meteorologist stationed at El Paso, directed the 1950 field operations. Mr. G. W. Farnsworth, Assistant Engineer, had the responsibility for the design and construction of modifications to the radar and for maintenance of the equipment, and for some of the analysis of the data collected. Much of the processing of the data was done by Mr. Homer Hiser, a graduate assistant. Dr. H. R. Byers, Meteorologic Consultant, contributed many valuable suggestions.

APPENDIX

Table 1

EFFECT OF GAGE DENSITY ON AREA-DEPTH CURVES
FOR INDIVIDUAL STORMS
40 GAGES VS. 20 GAGES, 95-SQUARE-MILE AREA
(Assuming 40 Gages or 2. 4 Sq. Mi. /Gage Gave True Mean)

	Area (square miles)					40-Gage
Storm Date	10	25	50	75	95	Mean Rainfall (inches)
	(Difference, Per Cent)*					
7/16-17/50	+2	+2	+2	+2	+2	5. 09
6/18-19/50	-3	-2	0	0	0	2. 56
9/20/50	-1	-1	-1	-1	-1	1. 92
7/19/50	-2	-2	-1	0	0	1. 29
9/19/50	-3	-2	0	+1	+1	1. 04
6/13/50	-1	+1	+3	+1	+1	1. 01
6/15/50	-1	-1	-1	-2	-2	. 82
6/24/50	-7	-7	-5	0	-1	. 66
Mean	3	2	2	1	1	
Maximum	7	7	5	2	2	

*Difference (per cent) = $\frac{\text{20-Gage Mean Rainfall - 40-Gage Mean Rainfall}}{\text{40-Gage Mean Rainfall}} \times 100$

Table 2

EFFECT OF GAGE DENSITY ON AREA-DEPTH CURVES
INDIVIDUAL STORMS. 95-SQUARE-MILE AREA
(Assuming 20 Gages or 4. 75 Sq. Mi. /Gage Gave True Mean)

	20-Gage Mean Rainfall	*Gage Density = 9. 5 Area (square miles)				Gage Density = 19. 5 Area (square miles)		
Date	(inches)	10	25	50	95	25	50	95
		(Difference, per cent)				(Difference, per cent)		
7/16/50	5. 22	-3	-2	-2	0	-15	-14	-8
6/13/49	2. 84	+2	+3	+3	+1	0	+1	+1
6/18/50	2. 57	-4	-2	-1	0	-1	-1	0
7/21/49	2. 31	-3	-3	-3	0	-5	-4	0
9/20/50	1. 90	+4	+5	+3	+4	-9	-6	-8
7/25/48	1. 84	-3	-3	-3	-3	-8	-5	-1
7/13/48	1. 68	-4	-4	-4	-3	-6	-3	+1
7/19/50	1. 29	+6	+7	+6	+2	+2	0	-6
6/26/48	1. 19	-11	-10	-6	0	-12	-12	-12
9/19/50	1. 04	+11	+11	+4	+1	-4	-2	-1
6/13/50	1. 02	-2	-4	-8	-6	-3	-2	-1
7/22/48	1. 00	+1	0	-1	-2	-4	-3	-3
6/23/48	. 93	-10	-6	-3	+2	-13	-11	-6
6/15/50	. 90	+1	+4	+6	+5	-7	-3	+4
6/24/50	. 65	-22	-11	-7	-9	-10	-10	-9
Mean		6	5	4	3	7	5	4
Maximum		22	11	8	9	15	14	12

*Gage Density = Average Area, Square Miles, per gage (10 gages = 9. 5, 5 gages = 19. 5 sq. mi. per gage).

Table 3

PERCENTAGE AREA-DEPTH COMPARISONS FOR DIFFERENT LOCATIONS
OF STORM RAINFALL CENTER WITH RESPECT TO BASIN AXIS
100-SQUARE-MILE RECTANGLE (12 x 8. 3) JULY 16-17, 1950 STORM

Rainfall Center with Respect to Basin Axis	Date	10	25	50	75	100	Rainfall Duration (hours)	Mean Rainfall (inches)
		(percent of basin mean rainfall)						
1. Coinciding with basin major axis	16-17	118	113	108	104	100	15	5. 30
	16	128	124	116	108	100	3	2. 43
2. Coinciding with basin minor axis	16-17	123	117	110	105	100	15	5. 06
	16	139	133	122	111	100	3	2. 22
3. Coinciding with basin boundary parallel to major axis	16-17	125	120	114	108	100	15	4. 77
	16	156	147	132	115	100	3	1. 93

Table 4

PERCENTAGE AREA-DEPTH RELATIONSHIPS, DIFFERENT STORM DURATIONS
RAINFALL CORES NEAR AREA CENTER
95-SQUARE-MILE BASIN, 1948-1950

Date	Area (square miles) 10	25	50	75	95	Mean Rainfall (inches)	Rainfall Duration (hours)
Storm Duration over 12 Hours							
7/16-17/50	120	115	109	104	100	5.22	15
6/13-14/49	119	112	106	103	100	2.84	14
6/18-19/50	115	111	106	102	100	2.57	18
Average	117	113	107	103	100		
Storm Duration 6-12 Hours							
7/17/50	132	124	114	106	100	2.77	9
6/14/49	120	113	106	103	100	2.02	8
7/25/48	130	125	116	107	100	1.84	6
6/19/50	123	115	107	103	100	1.43	12
6/18/50	128	120	111	104	100	1.14	6
Average	127	119	111	105	100		
Storm Duration Less than 6 Hours							
7/16/50 (3)	144	133	119	108	100	2.20	3
7/21/49	159	141	122	109	100	1.31	4
7/17/50 (1)	144	129	114	106	100	1.26	3
7/17/50 (2)	142	132	120	109	100	1.14	3
6/23/48	137	126	116	107	100	.93	3
6/26/48	158	141	124	110	100	.92	1
Average	147	134	119	108	100		

(1) First shower period, 17th.
(2) Third shower period, 17th.
(3) Second shower period, 16th.

Table 5

COMPARISON OF
AVERAGE PERCENTAGE AREA-DEPTH RELATIONSHIPS
IN STORMS WITH RAINFALL CORES NEAR BOUNDARY
WITH THOSE HAVING CORES NEAR BASIN CENTER

Type	Area (square miles) 10	25	50	75	95	No. Cases
	(percent of mean rainfall)					
1. Boundary	166	145	125	111	100	14
2. Center	147	134	119	108	100	6
3. Difference (1-2)	19	11	6	3	0	

Table 6

PERCENTAGE AREA-DEPTH RELATIONSHIP
PARTIAL STORM PERIOD VS. TOTAL STORM PERIOD
JULY 16-17. 1950

Storm Period	Area (square miles) 10	25	50	75	95	Mean Rainfall
	(percent of mean rainfall)					
1. First Storm (17th)	144	129	114	106	100	1.26
2. Second Storm (17th)	193	170	142	119	100	.37
3. Third Storm (17th)	142	132	120	109	100	1.14
4. Total (17th)	132	124	114	106	100	2.77
5. Total (16th-17th)	120	115	109	104	100	5.22

Table 7

PERCENTAGE AREA-DEPTH COMPARISONS
5.2-, 95-, 280-SQUARE-MILE BASINS
RAINFALL CORES NEAR AREA CENTER
(Storm Durations under 6 Hours)

5.2-Square-Mile Basin

Date	Area (square miles) 1	2	3	4	5.2	Basin Mean Rainfall	Rainfall Duration (hours)
7/17/50	108	107	106	104	100	2.38	1.5
6/28/49	119	115	110	105	100	1.11	3.
7/19/49	109	104	102	101	100	.94	0.5
Mean	112	109	106	103	100		

95-Square-Mile Basin

Date	Area (square miles) 10	25	50	75	95	Basin Mean Rainfall	Rainfall Duration (hours)
7/16/50	144	133	119	108	100	2.20	3
7/21/49	159	141	122	109	100	1.31	4
7/17/50	144	129	114	106	100	1.26	3
7/17/50	142	132	120	109	100	1.14	3
6/23/48	137	126	116	107	100	.93	3
6/26/48	138	141	124	110	100	.92	1
Mean	147	134	119	108	100		

280-Square-Mile Basin

Date	Area (square miles) 25	50	100	200	280	Basin Mean Rainfall	Rainfall Duration (hours)
7/21/49	184	170	152	123	100	1.06	4
6/26/48	174	165	150	122	100	1.01	2
6/23/48	176	160	141	116	100	.90	3
5/25/49	175	161	146	119	100	.59	2
6/25/49	175	163	148	119	100	.52	1
Mean	177	164	147	120	100		

Table 8

COMPARISON OF
AVERAGE PERCENTAGE AREA-DEPTH RELATIONSHIPS
STORMS HAVING RAINFALL CORES NEAR BASIN BOUNDARY
VS. STORM CORES NEAR BASIN CENTER
5.2-, 95-, 280-Square-Mile Basins

5.2-Square-Mile Basin						
	Area (square miles)					No.
Storm Type	1	2	3	4	5.2	Cases
Center	112	109	106	103	100	3
Boundary	125	117	113	107	100	15
Difference	13	8	7	4		

95-Square-Mile Basin						
	Area (square miles)					No.
Storm Type	10	25	50	75	95	Cases
Center	147	134	119	108	100	6
Boundary	166	145	125	111	100	14
Difference	19	11	6	3		

280-Square-Mile Basin						
	Area (square miles)					No.
Storm Type	25	50	100	200	280	Cases
Center	177	164	147	120	100	5
Boundary	193	174	148	120	100	11
Difference	16	10	1	0		

Table 9

PERCENTAGE AREA-DEPTH RELATIONSHIPS
RAINFALL CORES NEAR AREA CENTER
(Rainfall Duration 6 Hours or More)

	Area (square miles)					Mean Rainfall	Rainfall Duration
Date	25	50	100	200	280	(inches)	(hours)
6/13/49	122	118	113	105	100	2.88	14
6/14/49	128	123	116	107	100	1.97	8
7/25/48	143	136	125	111	100	1.77	6

Table 10

MEAN STORM RAINFALL DIFFERENCES
40 GAGES VS. 20 GAGES
95-SQUARE-MILE WATERSHED, 1950

Mean Rainfall Interval	No. Cases	Mean Differences	Maximum Differences
.01"-.50"	17	.014"	.04"
over .50"	10	.026"	.06"

Table 11

RELATION BETWEEN MEAN STORM RAINFALL AND MEAN ERROR
FOR DIFFERENT GAGE DENSITIES
95-SQUARE-MILE AREA, 1948-1950

Mean Rainfall (inches)	Number of Cases	Gage Density (square miles per gage)							
		9.5	19.5	32	95	9.5	19.5	32	95
		Mean Error (inches)				Mean Error (percent)			
.01- .20	23	.015	.019	.023	.050	14	19	23	50
.21- .50	20	.022	.028	.052	.088	6	8	15	27
.51-1.00	16	.028	.040	.090	.140	4	5	12	20
1.01-3.00	12	.045	.055	.130	.250	3	4	8	16

Table 12

FREQUENCY DISTRIBUTION OF ERRORS FOR DIFFERENT GAGE DENSITIES
ASSUMING 20 GAGES (4.75 SQUARE MILES PER GAGE)
GAVE TRUE MEAN RAINFALL, 95-SQUARE-MILE
AREA, 1948-1950

Gage Density (sq. mi./gage)	Maximum Error		Percent of Cases Error Equal to or Less than Indicated Value in Column					
	(inches)	(percent)	25%	50%	75%	25%	50%	75%
			Error (inches)			Error (percent)		
Mean Storm Rainfall, .01"-.20"								
9.5	.06	40	.01	.01	.02	6	11	20
19.5	.08	57	.01	.01	.03	9	16	25
32	.09	67	.01	.02	.03	8	15	25
95	.24	240	.01	.03	.06	16	29	50
Mean Storm Rainfall, .21"-.50"								
9.5	.18	38	.01	.02	.03	3	5	9
19.5	.10	35	.01	.02	.04	3	5	11
32	.28	60	.01	.02	.06	4	8	24
95	.39	105	.02	.07	.13	5	23	33
Mean Storm Rainfall, .51"-1.00"								
9.5	.09	13	.01	.02	.04	1	4	8
19.5	.11	17	.01	.04	.05	2	6	8
32	.29	42	.02	.08	.10	2	11	16
95	.31	59	.06	.13	.19	6	13	29
Mean Storm Rainfall, 1.01"-3.00"								
9.5	.16	9	.01	.03	.07	1	2	7
19.5	.13	12	.01	.03	.07	1	2	3
32	.28	20	.05	.15	.19	2	8	11
95	.49	36	.10	.22	.40	7	13	22

Table 13

RELATION BETWEEN MEAN MONTHLY AND SEASONAL RAINFALL
AND COMPUTATION ERROR FOR DIFFERENT GAGE DENSITIES
95-SQUARE-MILE AREA, 1948-1950
(Assuming 20 Gages or 4. 75 Square Miles per Gage Gave True Mean)

Month	20-Gage Mean Rainfall (inches)	Error for Indicated Gage Density (square miles/gage) 9.5 (10 gages) (inches)	(%)	19.5 (5 gages) (inches)	(%)	32 (3 gages) (inches)	(%)	95 (1 gage) (inches)	(%)
June 1948	3.96	-.07	-2	-.13	-3	-.15	-4	-.04	-1
July 1948	6.61	+.05	+1	+.01	0	-.27	-4	+.26	+4
August 1948	1.19	-.06	-5	+.04	+3	+.12	+10	+.29	+24
June 1949	4.41	-.01	0	-.08	-2	-.33	-7	+.19	+4
July 1949	4.67	-.32	-7	-.22	-5	-.39	-8	-.21	-4
August 1949	1.60	-.05	-3	-.08	-5	-.07	-4	+.09	+6
June 1950	6.40	-.03	-1	+.22	+3	-.32	-5	+.26	+4
July 1950	6.72	-.11	-2	-.41	-6	-.33	-5	-.65	-10
August 1950	0.57	+.05	+9	+.04	+7	-.02	-4	-.12	-21
Average Error		.08	3	.14	4	.22	6	.23	9
June-August 1948	11.76	-.08	-1	-.08	-1	-.30	-3	+.51	+4
June-August 1949	10.83	-.38	-4	-.38	-4	-.80	-7	+.08	+1
June-August 1950	13.69	-.09	-1	-.15	-1	-.67	-5	-.51	-4

Table 14

AREAL MEAN RAINFALL VS. STORM TYPE

Storm Type	Number of Storms	Percent of Total Storms	Rainfall Amount (inches)	Percent of Total Areal Rainfall	Maximum Individual Storm (inches)
Cold front	49	38	18.66	40	2.02
Pre-cold frontal squall line	16	12	12.42	26	2.77
Warm front	30	23	10.74	23	2.56
Warm air mass instability	30	23	5.28	11	0.76
Cold air mass instability	5	4	0.12	0.3	0.05
Cold front plus squall line	65	50	21.08	66	

Table 15

AREAL MEAN RAINFALL VS. STORM TYPE
STORM RAINFALL EQUAL TO OR
GREATER THAN 0. 50" AND 1. 00"

Storm Type	Number of Storms		Percent of Total Storms	
	0. 50"	1. 00"	0. 50"	1. 00"
Cold front	13	5	42	50
Pre-cold frontal squall line	9	3	29	30
Warm front	5	2	16	20
Warm air mass instability	4	0	13	0
Cold air mass instability	0	0	0	0
Cold front plus squall line	22	8	71	80

Table 16

EXCESSIVE RAINFALL RATES VS. STORM TYPE
.30-MINUTE, 1-HOUR, AND 2-HOUR PERIODS

Storm Type	Number of Storms*			Percent of Total Storms		
	30-Minute	1-Hour	2-Hour	30-Minute	1-Hour	2-Hour
Cold front	13	11	5	52	58	56
Pre-cold frontal squall line	6	5	3	24	26	33
Warm front	2	2	1	8	11	11
Warm air mass instability	4	1	0	16	5	0
Cold air mass instability	0	0	0	0	0	0
Cold front plus squall line	19	16	8	76	84	89

*Number of storms in which one or more stations recorded excessive rates.

Table 17

30-MINUTE AMOUNTS EXCEEDING 1. 0 INCH

Storm Type	Number of Storms	Percent of Total Storms
Cold front	4	50
Pre-cold frontal squall line	3	38
Warm front	1	12
Warm air mass instability	0	0
Cold air mass instability	0	0
Cold front plus squall line	7	88

Table 18

SUMMARY OF RADAR-RAINFALL DATA

Month & Date	Year	Radar Time	Precipitation Time	Rainfall Drift (miles and direction)	Radial	$P_r \times 10^{-12}$ (watts)	Surface Rainfall Rate (in./hr.)	Range (K-miles)	$\frac{P_r R^2}{P_t \times 10^{-16}}$
Sept. 19	1950	0838.5	0839	3/4 SE	4	7.4	.06	14.4	0.045
						35.5	.42	16.3	0.250
						160.	.48	16.5	1.250
						1100.	.60	16.7	8.80
					5	7.4	.06	13.2	0.040
						35.5	.12	14.1	0.200
						160.	.18	14.2	0.980
						1100.	.30	14.3	6.800
					6	160.	.06	13.9	0.950
						1100.	.24	14.3	6.800
						5000.	.48	14.6	30.500
Sept. 19	1950	0915	0918	1/4 NE	8	7.4	.06	16.7	0.058
						35.5	.12	17.0	0.270
						160.	.30	17.5	1.350
						1100.	.36	17.7	9.800
					6	35.5	.12	18.5	0.315
						160.0	.36	18.8	1.550
						1100.	.60	19.4	12.000
Sept. 19	1950	0845.5	0847.5	1 1/4 E	6	7.4	.06	12.4	0.036
						35.5	.12	14.2	0.200
						160.	.24	15.3	1.100
						1100.	.30	15.4	7.600
						5000.	.42	16.0	35.500
Sept. 19	1950	0918	0920	1 1/4 SE	7	7.4	.12	17.6	0.064
						35.5	.18	18.0	0.300
						160.0	.24	18.3	1.450
						1100.	.30	18.5	11.000
Sept. 19	1950	0916.5	0919	3/4 SE	6	7.4	.12	18.3	0.068
						35.5	.12	18.5	0.315
						160.	.24	18.9	1.550
						1100.	.30	19.0	11.500
Sept. 19	1950	0818	0820.5	0	5	35.5	.24	13.7	0.190
						160.	.48	16.5	1.200
						1100.	.60	17.0	9.100
						5000.	.66	17.1	40.000
Sept. 19	1950	0835.5	0837.5	1 SE	5	35.5	.35	14.9	0.220
						160.	.42	15.3	1.100
						1100.	.48	15.7	7.900
Sept. 19	1950	0840.5	0841.5	1/2 E	5	35.5	.30	14.9	0.220
						160.	.36	15.6	1.100
						1100.	.54	16.2	8.400
Sept. 19	1950	0844.5	0846.5	1/2 N	5	160.	.36	15.7	1.150
						1100.	.56	16.2	8.400
						5000.	.60	16.5	37.500
Sept. 19	1950	0819.5	0822.5	1/2 SE	5	160.	.12	15.3	1.100
						1100.	.54	17.0	8.700
						5000.	1.02	18.0	40.000
					7	160.	.30	15.8	1.150
						1100.	.54	16.5	8.600
Sept. 20	1950	1024	1026	0	4	7.4	.06	14.9	0.0475
						35.5	.12	15.3	0.225
						160.	.18	15.4	1.100
						1100.	.24	15.6	7.800
					2	35.5	.30	16.2	0.250
						160.	.54	16.4	1.200
						1100.	.60	16.6	8.700
						5000.	.66	16.8	39.000
Sept. 20	1950	1024	1026	0	3	35.5	.24	15.6	0.230
						160.	.42	15.7	1.150
						1100.	.54	15.9	8.000
						5000.	.66	16.1	36.000
Sept. 20	1950	1027	1029	0	3	7.4	.12	14.7	0.0465
						35.5	.30	15.1	0.220
						160.	.42	15.2	1.100
						1100.	.54	15.3	7.500
Sept. 20	1950	1029.7	1032	1/4 S	2	7.4	.12	14.5	0.046
						35.5	.18	14.6	0.210
						160.	.24	14.8	1.050
						1100.	.36	15.0	7.300
						5000.	.60	15.4	33.000
					3	1100.	.30	14.5	6.900
						5000.	.48	14.7	30.500
Sept. 20	1950	1025	1027	1/2 S	3	35.5	.12	15.5	0.230
						160.	.24	15.6	1.100
						1100.	.42	15.8	8.000
						5000.	.60	16.0	35.500
Sept. 20	1950	1030.7	1033	1 N	2	7.4	.18	14.3	0.044
						35.5	.18	14.5	0.205
						160.	.60	14.7	1.050
						1100.	.90	15.0	7.300
						5000.	1.02	15.4	30.000
					3	160.	.42	14.0	0.960
						1100.	.54	14.2	6.700
						5000.	.84	14.6	30.000

LIST OF REFERENCES

1. The Thunderstorm, Report of the Thunderstorm Project (A Joint Project of Air Force, Navy, National Advisory Committee for Aeronautics, Weather Bureau), Horace R. Byers, Director, Roscoe R. Braham, Jr., Senior Analyst, U. S. Department of Commerce, Weather Bureau, Washington, D. C., June 1949.

2. Hydrometeorological Report No. 5, Thunderstorm Rainfall, U. S. Department of Commerce, Weather Bureau, and U. S. War Department, Corps of Engineers, 1947.

3. Langhein, W. B., "Error in Computation of Mean Areal Precipitation," U. S. Geological Survey, Mimeograph, August 1946.

4. Linsley, Ray K. and Kohler, Max A., "Variations in Storm Rainfall over Small Areas," U. S. Department of Commerce, Weather Bureau (to be published).

5. M. L T. Weather Radar Research, 1946. First Technical Report under Signal Corps Project, M. I. T. Department of Meteorology, December 31, 1946.

6. Swingle and Wexler, Preliminary Report on Optimum Wave-length for Storm Detection, Technical Memorandum No. 183-R, Evans Signal Laboratories, November 7, 1945.

7. Weinstein and Wexler, Rainfall Intensities and Attenuation of Centimeter Electromagnetic Waves, Evans Signal Laboratories, 1947.

8. Brooks, H. B., Ground Weather Test of AN/APQ-13A, Technical Memorandum No. 193-R, Evans Signal Laboratories April 17, 1946.

9. Ryde, J. W., The Attenuation and Radar Echoes Produced at Centimeter Wave-lengths by Various Meteorological Phenomena, The Physical Society and the Royal Meteorological Society, Report of a Conference held on April 8, 1946, pp. 169-189, April 1946.

10. Marshall, J. S., Langille, R. C., and Palmer, W. McK., Measurement of Rainfall by Radar, Journal of Meteorology, Volume 4, No. 6, pp. 186-192, December 1947.

11. Byers, H. R. and Collaborators, The Use of Radar in Determining the Amount of Rain Falling Over a Small Area, Transaction American Geophysical Union, Volume 29, No. 2, pp. 187-196, April 1948.

12. Atlas, D., Preliminary Report on New Techniques in Quantitative Radar Analysis, Memorandum Report AWNW 7-4, Part I, All-Weather Flying Division, AMC, U. S. A. F., October 22, 1947.

13. Stratton, J. A., The Effect of Rain and Fog on the Propagation of Very Short Radio Waves, Proceedings of the Institute of Radio Engineers, Volume No. 6, pp. 1064-1074, June 1930.

14. Laws, J. O. and Parsons, D. A., The Relation of Raindrop-Size to Intensity, Transactions American Geophysical Union, Volume 24, Part II, pp. 452-459, 1943.

15. Wexler, R., Radar Detection of a Frontal Storm June 18, 1946, Journal of Meteorology, Volume 4, pp. 38-44, February 1947.

16. Atlas, D., Some Experimental Results of Quantitative Radar Analysis of Rain Storms, Memorandum Report AWNW 7-4, Part II, All-Weather Flying Division, AMC, U. S. A. F., May 1, 1948.

17. Spilhaus, A. F., Drop Size, Intensity, and Radar Echo of Rain, Journal of Meteorology, Volume 5, No. 4, pp. 161-164, August 1948.

REPORTS OF INVESTIGATIONS
ISSUED BY THE STATE WATER SURVEY

No. 1. Temperature and Turbidity of Some River Waters in Illinois. 1948.

No. 2. Groundwater Resources in Winnebago County, with Specific Reference to Conditions at Rockford. 1948.

No. 3. Radar and Rainfall. 1949.

No. 4. The Silt Problem at Spring Lake, Macomb, Illinois. 1949.

No. 5. Infiltration of Soils in the Peoria Area. 1949.

No. 6. Groundwater Resources in Champaign County. 1950.

No. 7. The Silting of Ridge Lake, Fox Ridge State Park, Charleston, Illinois. 1951.

No. 8. The Silting of Lake Chautauqua, Havana, Illinois. 1951.

No. 9. The Silting of Carbondale Reservoir, Carbondale, Illinois. 1951.

No. 10. The Silting of Lake Bracken, Galesburg, Illinois. 1951.

No. 11. Irrigation in Illinois. 1951.

No. 12. The Silting of West Frankfort Reservoir, West Frankfort, Illinois. 1951.

No. 13. Studies of Thunderstorm Rainfall with Dense Raingage Networks and Radar. 1952.